

Dr. Olaf Eisen, Editor

Dear Dr. Eisen,

A response to comments from the two reviewers of this manuscript are provided below (in blue text), along with tracked to the manuscript and supplementary material. A small change was made to our method of calculating the peaks in seasonal cycles of mass change, which necessitated redoing some of the figures. However, the results and conclusions are essentially the same. Thanks very much for overseeing the review of this manuscript.

Sincerely,
Patrick Alexander
(On behalf of all co-authors)

Response to Reviewer 1:

Interactive comment on “Greenland Ice Sheet seasonal and spatial mass variability from model simulations and GRACE (2003-2012)” by P. M. Alexander et al.

Anonymous Referee #1

The manuscript is a valuable contribution on our current degree of understanding mass changes of the Greenland Ice Sheet on regional spatial scales and seasonal temporal scales. Mass variations derived from GRACE Level-1 data by the mascon method of Lutchke et al. are compared to modelled changes due to SMB and ice flow based on the MAR Regional Climate Model and the ISSM Ice sheet model. One of the merits of this work is the comprehensive explanation and illustration of the complex filtering associated to the GRACE mascon results and of the way how the GRACE-versus-modeling comparisons account for this filtering.

The manuscript is very well structured and well readable despite the technical nature of part of the discussion. The figures are excellent.

[We thank the reviewer for valuable comments and taking the time to read the manuscript carefully.](#)

I have just a few points.

An important point concerns the calculation of the seasonal cycles shown in many figures and introduced on p. 6360, line 4ff. It is unclear why (and how) a two-year composite seasonal cycle was constructed. Why not a one-year composite cycle? How does the two-year cycle relate to the one-year plots?

[We thank the reviewer for raising this point, which ultimately should improve the manuscript. We created a one-year average seasonal cycle for all regions as seen in](#)

all figures. In order to compute the maximum and minimum peaks in the cycle, a two-year cycle was created from the average one-year cycle in which the one-year cycle was repeated, with the second year beginning at the mass value of the previous year. This two-year “wrapping” of the cycle was deemed necessary because the first and last values of the average seasonal cycle are not identical, as the reviewer has noted below. This can occur as a result of non-linear variations in mass across multiple years, which are not removed when we de-trend the cumulative timeseries. In this instance, the change in mass during the winter months must be examined in the context of a “hydrological” year, which spans the winter months.

However, we now believe that this two-year wrapping is unnecessary because it is not necessary to constrain the values for December 31 and January 1 to be equivalent, as the average cycle reflects the average fluctuations across the entire period examined. Therefore, a wrapped seasonal cycle should return to the same mass value at the start of the second year. We have therefore simply computed the maximum and minimum values from the one-year average cycle, and have adjusted all figures accordingly. This change, along with the addition of ± 10 days in error bars to account for errors associated with temporal resolution, have caused the timing of seasonal cycles and uncertainty ranges to shift somewhat. As a result the GrIS sub-regions derived from the timing of seasonal cycles are also slightly different (Fig. 11a). We slightly adjusted the threshold on seasonal cycle timing from 30 to 34 days (Section 3.4) to produce a similar number of ice sheet sub-regions with distinct patterns of mass change. There are now nine sub-regions rather than eight, but the clustering of the regions is similar, with similar patterns of mass change. All figures that depict mass changes within the sub-regions have been updated, and portions of the results section have been adjusted in accordance with the changes, but our results and conclusions regarding the timing of mass changes in different regions have remained the same.

Seasonal cycles shown in plots like Fig. 8b, Fig 11d,e etc. sometimes show very different values at the left end and the right end of the plot, although both values are to represent Dec. 31 and Jan 1, respectively. Since the paper is on the seasonal cycles, it is important that the way of deriving these cycles be explained in more detail.

Further details have been added in the text (Section 2.4.4) discussing how the seasonal cycle is calculated and analyzed, as noted above. The method of deriving the seasonal cycle is fairly simple, however, and has already been noted in Section 2.4.4. We simply take the cumulative mass timeseries, interpolated to daily timesteps, for the region being examined, remove the 2003-2012 linear trend from this timeseries, and for each day of the year, take the average of the cumulative mass value for this day across all years. The values on January 1 and December 31 can be different due to non-linear fluctuations in the original timeseries. In particular, the high mass-loss year of 2012 likely reduces the average values towards the end of the year within some basins.

As we are primarily interested in comparing the models with GRACE-LM, we do not attempt to correct for non-linear interannual mass variations, which would be difficult to separate from seasonal variations. Non-linear variations in mass, and interannual variations in the seasonal cycle may contribute to some of the differences between GRACE-LM and the models, as we have noted in Section 4. For the purposes of this study we are mainly interested in identifying discrepancies between the models and GRACE-LM with respect to the average cycle across all years.

Section 2.4.4 has been updated as follows:

“We examined differences between the modeled and GRACE-LM seasonal cycles of cumulative mass change by first linearly interpolating filtered cumulative model and GRACE-LM timeseries onto daily timesteps. This was necessary because the GRACE-LM timesteps are not evenly spaced, and do not occur at the same point in time every year. We then subtracted the long-term linear trend for the entire timeseries (2003-2012) obtained from least-squares regression, to remove the impact of differences in trends on the timing of the seasonal cycle. After removing trends, the cumulative mass value for a given day of the year was averaged across all years in the 2003-2012 period, to yield an average annual cycle for all years. The maximum and minimum peaks were computed from this average annual cycle. This was performed for the GrIS-wide timeseries, as well as for individual mascons and GrIS sub-regions.”

The authors do an excellent job in describing the complex filtering inherent to the GRACE mascon solutions. The figures illustrate that the GRACE processing may, to some degree, distort (not just smooth) the spatial pattern of signals. Most remarkably, Fig. 1 illustrates that the partitioning of GRACE mascons into mascons below and above 200m elevation does not precisely match the limits between distinct regimes of modelled SMB and dynamically induced mass balance. The authors could somewhat more account for these limitations when discussing the GRACE-versus-modeling results later-on in the manuscript.

The GRACE-LM processing does not involve “filtering”, in the sense that observations of mass change are spatially smoothed or modified through processing. Rather the processing serves to estimate the mass changes within individual mascons given the observed KBRR data from the GRACE satellites. The resulting derived pattern of mass changes is in a sense spatially smoothed and distorted because the mascons are spaced at a distance that is smaller than the fundamental spatial resolution of GRACE. For this reason, it is necessary to apply a filter to our model outputs for comparison with the GRACE solution.

The objective of using the constraint regions is to reduce the “smoothing” effect to concentrate ice sheet mass loss into areas where it is known that mass loss is occurring. Certainly the 2000 m elevation boundary is not a perfect dividing line between high and low elevations, and future GRACE solutions may employ more

complex methods to better capture spatial variability of mass changes. We conduct filtering on model results for the purpose of comparing the models with GRACE subject to the same kind of spatial patterns from GRACE-LM and are more interested in the comparison between GRACE-LM and models filtered to match the GRACE solution. But we agree that in the cases the reviewer has mentioned there should be further clarification, and have reiterated that model results being compared with the GRACE-LM solution are filtered, and therefore the model results are spatially smoothed and to some extent, distorted.

For example, on p. 6367, they write: “the timing of GRACE-LM peaks tends to be clustered in groups, suggesting that the spatial variations in GRACE-LM timing are not random.” It could be discussed whether the observed clustering could be a consequence of the GRACE-LM filtering effect, even if its actual origin is “random”.

Indeed, one would expect clustering in the GRACE results, given that changes within two adjacent mascons are influenced by mass changes occurring in overlapping regions. This is a function of GRACE-LM spatial resolution. The regularization matrix used in the GRACE-LM processing constrains nearby mascons to exhibit a similar signal. However, there are differences between adjacent mascons, and such variations could potentially lead to differences in timing between mascons. The fact that there is a widespread discernable signal in the GRACE data suggests that there is a real signal in this region that is large enough to be detected by GRACE. We leave open the possibility that processes not related to ice sheet mass change, not accounted for in the GRACE processing could lead to the observed differences, although it is unclear what these processes might be. We discuss this further in response to the reviewer’s comment about p. 6368, l. 28.

The sentence has been revised to read:

“The clustering of the GRACE-LM peaks, despite the large uncertainty in the GRACE timing, suggests that the observed variations in timing are not associated with random deviations between mascons, but reflect seasonal variations in mass detected by GRACE-LM, that are not captured by the models.”

Likewise, when discussing the GRACE-versus-modeling differences in the zone above 2000m (Fig. 12b) it could be pointed out that these differences could well originate from modeling errors for regions *below* 2000m (given much higher signal amplitudes there), which may leak into the high-elevation results.

The purpose of the constraint regions is to minimize the leakage between areas above and below 2000 m to produce a more realistic signal for areas above 2000 m in elevation. Leakage across the constraint regions is therefore small; the impact on annual amplitude of the signal is on the order of the magnitude of estimated error (Luthcke et al., 2013). It is possible that the Gaussian filtering overestimates leakage, although the good agreement between GRACE-filtered and Gaussian-filtered model outputs (Fig. 3) suggests otherwise. We have noted that leakage from other regions may contribute to the differences, but that we expect the impact is small.

The end of Section 3.4 has been modified to take into account the potential influence of lower elevation changes on higher elevation fluctuations, and the following sentence has been added:

“Accumulation or ice flow errors could also affect differences at higher elevations, where the net ablation due to melting is small (i.e. above 2000 m in elevation). Such discrepancies could also be influenced by differences below 2000 m due to leakage between constraint regions, but the amount of leakage in terms of amplitude is small and is comparable to the GRACE-LM uncertainty (Luthcke et al., 2013).”

p. 6369, line 4f: It is not clear to what result or figure the “early start to the period of mass loss in the northeast from November through February” refers. Similarly, on p. 6732, it is not clear to what result the mention of “northeast Greenland” refers.

We meant to refer to “northwest Greenland” rather than “northeast Greenland”. “Northeast” has been changed to “northwest” in both cases, and we now refer to Fig. 9a-c on p. 6369.

Minor points:

I was initially confused about the use of MAR v2.0 versus MAR v3.5.2. Maybe it could be mentioned at an early place that the comparison with GRACE is ultimately done for v3.5.2, while MAR v2.0 is used to assess different filters because the numerically most expensive filter was previously applied to v2.0 but not to v3.5.2.

We have added an explanation about this at the end of Section 2.2, where the MAR model outputs are introduced.

p. 6357, line 11 “A different σ_i value is chosen for each mascon”: Maybe add “as explained below”, to keep the reader patient about an explanation. We have added the phrase “as will be explained further below.” to the end of the sentence, as suggested.

There is an unnecessary repetition about how λ_{ij} are define, before and after Equation 8. Instead you could add “as explained below” again, to keep the reader patient about the mystery of these coefficients.

Agreed. The text has been changed as suggested.

p. 6358, line 21: Symbol σ_l was not introduced before. Please homogenize annotation.

We incorrectly used an uppercase “I” here. It’s been changed to a lowercase “i”.

Line 6360 last line. For better clarity, write “GRACE-LM *filtering* vs. Gaussian filtering”

This has been changed as suggested.

p. 6364, line 17ff. It is not clear why the discussion concentrates on the region where ISSM underestimates ice thickness and it cannot be seen from any figure that ISSM underestimates ice velocities at these places.

Figure S4b suggests that ISSM underestimates ice velocities for glaciers along the northwest coast of the GrIS. These the thicknesses along the coast at these glaciers appears to be overestimated (Fig. S4b), but the thickness upstream of the glaciers is underestimated, possibly contributing to the underestimated velocities. We have added further discussion of spatial variations in differences between ISSM and observations, and how this may relate to the differences between ISSM + MAR v3.5.2 and GRACE on p. 6364:

“In particular, ice velocities tend to be underestimated for glaciers along the northwest coast of the GrIS (Fig. S4b), possibly as a consequence of an upstream ice thickness that is also underestimated (Fig. S4a). This may contribute to underestimated mass loss along the northwest coast. In other areas, ice thickness is generally overestimated by ISSM, but some outlet glacier velocities are overestimated while others are underestimated, making it unclear how ISSM contributes to the observed discrepancies in these regions.”

p. 6364, line 23. Avoiding the SSA acronym (used at only one occasion) would make the text more readable.

We have replaced the SSA acronym with the “Shelfy Stream Approximation” for clarity and have removed the SSA acronym from Section 2.3.

p. 6370, lines 3-4: Please clarify. It is not clear to me what “it” and “The Greenland-Wide cycle” refer to.

We agree that the sentence was confusing. We have replaced the sentence with the following:

“As the filter extends the length of the modeled period of mass loss, and tends to bring the timing of modeled seasonal cycle peaks closer to those from GRACE-LM (which exhibits a longer period of mass loss relative to the unfiltered model results), our approach is conservative: in cases where the cycles disagree, there is likely a difference between the GRACE-LM and modeled seasonal cycles.”

Fig. 4 Caption “a temporal filter has not been applied”: The legend within the figure, instead, says “Gaussian(Spatial, *Time*) Filtered” for one of the curves.

The sentence in the caption was incorrect. It has been changed to read:

"Timeseries are shown for Gaussian filtered MAR v2.0 outputs subject to only spatial filtering (gray curve) and both spatial and temporal filtering (blue curve)."

Response to Reviewer 2:

Interactive comment on “Greenland Ice Sheet seasonal and spatial mass variability from model simulations and GRACE (2003-2012)” by P. M.

Alexander et al.

Anonymous Referee #2

Review of paper by Alexander et al.

General comment

The paper by Alexander et al. entitled “Greenland Ice Sheet seasonal and spatial mass variability from model simulations and GRACE (2003-2012)” employs surface mass balance from the regional climate model MAR v3.5.2 and the ice sheet model ISSM, to obtain a good representation of the overall Greenland Ice Sheet Mass Balance changes between 2003 and 2012. The authors process model outputs performing a spatio-temporal filtering in order to make a fair comparison with mass changes obtained from the GRACE data using the mascon strategy developed by Luthcke et al. (2013). They find a quite good agreement over the entire ice sheet and several sub-regions. Some discrepancies remain to date unexplained.

The paper is well written and illustrated. Succeeding in comparing GRACE and model outputs, the paper is a significant step towards the understanding of mass changes over the Greenland Ice Sheet but also at a more regional scale which is fundamental to understand the overall ice sheet system and its response to climate change.

[We thank the reviewer for taking the time to review the paper and for comments that improved the quality of the manuscript.](#)

Specific comments

p. 6359 – l. 26-27: “the Gaussian filtering procedure does not incorporate changes in mass”. It looks to me that it is not entirely correct, or I may have misunderstood the filtering strategy. Indeed, the parameters σ_I , λ_I and σ_t seem to be determined using “the aggregated unfiltered MAR v2.0 data”. However, leakage is usually a function of the mass change in mascon j and mascon j . So I wonder why the parameters mentioned above would not change using the aggregated unfiltered MAR v3.5.2 data given the differences mentioned in the manuscript between the two versions of the model. The entire GrIS MB may not significantly be affected because the differences between v2.0 and v3.5.2 of MAR may only result in the spatial distribution of the MB but not the total MB of the GrIS. However, for each mascon, MB might change from one model to another. Can you clarify this up?

[The choice of parameters for Gaussian filtering is determined through comparison between aggregated unfiltered MAR v2.0 data, to which Gaussian filtering is applied, and the GRACE-filtered MAR v2.0 data. The Gaussian filtering is a means of](#)

redistributing or smoothing the mass change from the unfiltered MAR v2.0 data in space and time so that the patterns of mass change from the Gaussian-filtered data match the GRACE-filtered patterns of mass change. It is therefore a way of approximating the effects of the GRACE resolution operator without a high degree of processing. The resolution operator is independent of the dataset to which it is applied, and therefore our derived parameters should also be independent of the dataset being filtered, since they depend not on the original mass change values from MAR v2.0 but on the relationship between the unfiltered and GRACE-filtered MAR v2.0 data. We should therefore be able to derive the same parameters using unfiltered and GRACE-filtered MAR v3.5.2 data. We have clarified this as follows:

“These differences do not affect our ability to filter MAR v3.5.2 outputs, as the Gaussian filter does not depend on mass changes, but approximates the GRACE-LM resolution operator, which serves to redistribute mass changes subject to specified constraint regions.”

p. 6360, l. 6: “to a daily temporal resolution” is not quite correct, you are not increasing the temporal resolution, you are just increasing the number of time sample which leads me to the question, can you really give in the following sections of your manuscript seasonal timing at a daily/weekly (p. 6365, l. 21: “roughly 1 week earlier”) accuracy given that GRACE-LM and GRACE-like filtered models have a time resolution of 10 days?

The resolution of the GRACE solution is roughly but not exactly 10 days. Therefore GRACE results are not provided on exactly the same day every year. For this reason it was necessary to interpolate the data to daily timesteps. The GRACE solution is therefore sampling the seasonal cycle on different days every year, reducing some of the error associated with the GRACE temporal resolution. The maximum error in timing associated with a peak is roughly 10 days, but this is nearly always smaller than the range of timing that we have estimated from the uncertainty in GRACE data. Given the relatively large uncertainty on GRACE outputs, we generally provide the median date or likely range of dates for the timing of GRACE peaks, and most of the differences discussed are larger than 1 month. We agree that we cannot say with certainty that there is a difference of 1 week between any two peaks. We have added an additional 10 days of uncertainty on each end of our error bars, have revised the text where necessary to avoid discussion of differences smaller than 10 days. The following text has been added to section 2.4.4:

“The temporal resolution of the GRACE-LM dataset can also lead to errors of roughly ± 10 days for the timing of any estimate. Because the GRACE-LM timesteps are not regular, the uncertainty on the timing of peaks for the average seasonal cycle due to temporal resolution is generally smaller than 10 days. Given that the error could be as large as 10 days, however, we calculated our error on the timing of seasonal cycle peaks as the 95% confidence interval from the Monte Carlo simulations, ± 10 days. If model peaks fell outside of this error range, the timing of the GRACE-LM and model peaks was deemed to differ.”

p. 6360, l. 8: “two-year composite seasonal cycle” why two years ? need justifications here.

See the response to the first general comment from Reviewer #1. A two-year wrapped seasonal cycle was constructed to calculate maximum and minimum values in the seasonal cycle. However, we now calculate the maximum and minimum values from the annual average seasonal cycle.

p. 6361, l. 2-8: As you say, “it is not possible to compare GRACE-derived mass changes directly to MAR” however you can compare MAR v3.5.2 with ISSM, so why not doing it earlier so that your assumption regarding ice discharge changes can be justified?

Because ISSM outputs are a model result, we do not feel that we can use the ISSM results as definite proof that variability in ice discharge is small relative to variability in SMB at this point in the manuscript, especially since the ISSM simulation does not include processes that may contribute to higher seasonal variability, such as the influence of meltwater on ice velocities and ice-ocean interactions. We agree that the model results do provide some support to this assumption, and have added this sentence to the discussion:

“(As will be seen in Section 3.2, modeled ice-sheet wide seasonal variability from ISSM is also less than 10% of variability from MAR.)”

p. 6368, l. 28: What type of GRACE errors might influence the variability in that context? Are, for instance, loading effects of surface mass changes of the GrIS and atmospheric changes taken into account when inverting for the KBRR data? Could it have an important impact on the signal, e.g. the amplitudes? Is the atmospheric model used in the GRACE-LM processing strategy the same as in the SMB model?

We have left open the possibility that some process unaccounted for might lead to the observed variability, but we do not believe that the processes taken into account in processing of GRACE data could have an impact on this variability, and their estimated uncertainty is taken into account in the calculation of uncertainty for each mascon. Loading effects of surface mass changes are not expected to have an impact on variability at the relatively short timescales examined here. Uncertainty associated with the atmospheric and ocean models used in the GRACE processing are estimated from differences between two different sets of models (as discussed by Luthcke et al., 2013). Given relatively sparse data for validation in this region, it is possible that model errors are larger than the inter-model differences, but we do not know what the magnitude of these errors might be. The atmospheric model used in GRACE-LM processing is the ECMWF reanalysis, which is the reanalysis used to drive MAR at the lateral boundaries. As ECMWF is used for estimating variations in atmospheric pressure, while MAR is used to estimate SMB, it seems unlikely that the use of ECMWF vs. another model could substantially impact the observed

differences. We have clarified in the text in section 3.4 that we do not know of any likely source for the differences, but leave open the possibility that some unknown factor could be responsible:

“Additionally, it is possible that although the GRACE-LM solution includes error estimates associated with the forward models used in GRACE processing, unaccounted for errors or processes, such as errors in model simulations used to correct for variability in atmospheric or ocean circulation (for which observations for validation are limited) may contribute to the differences. However, we cannot envision any obvious reason for the discrepancy other than the potential errors in ISSM or MAR v3.5.2 that have been noted.”

Technical corrections

p. 6347

l. 4f: “While several studies...are still lacking.” A short sentence to explain why it is important to examine sub-annual and sub-basin-wide changes would be nice here.

We have added a short sentence as suggested:

“At these scales, processes responsible for mass change are less well understood and modeled, and could potentially play an important role in future GrIS mass change.”

p. 6349

l. 6-9: MB in l. 6 only defined in l. 9.

MB on l. 6 has been changed to “rate of GrIS mass change”

p.6350

l.4: you should precise the starting and ending months of the period of interest at least once but best everywhere the period appears.

We have added the starting and ending months when describing model simulations and GRACE outputs for the sections prior to the results, and for table and figure captions. In the results and conclusions sections we have left out the months for readability. Generally in all cases the period begins in January and ends in December, and we feel this is implied by the range of years. The only exception is the GRACE dataset, which begins in January 2003 and ends in June 2013. However, we have chosen to only consider data through 2012 in our analysis, as we are interested in capturing complete years for the purpose of evaluating the seasonal cycle. This has been clarified in Section 2.1. We have also revised Fig. 6 to include the only timeseries' through 2012, to avoid creating confusion, as all analysis is performed for the January 2003 – December 2012 period.

l. 15: “between GRACE-derived and simulated” -> would estimated be better than simulated here?

This sentence was confusing. We have replaced “simulated mass changes not accounted for by the simulations” with “modeled mass changes”.

p. 6352:

l. 4-5 you should precise the starting and ending months of the two mentioned periods.

These have been added as suggested.

p. 6353

l. 19-23: Following these lines I expected some results of the evaluation and the comparison just mentioned. Instead it comes much later (p. 6364). May worth to modify a little bit the text here for instance by moving these lines to p. 6364.

As suggested, we have moved this material to Section 3.1.

l. 24: Is the period 2003-2013 correct? Isn't it 2012? Can you also precise the starting and ending months please?

Indeed, the period is January 2003 – December 2012. We have corrected the text accordingly.

Could be nice for clarity to summarize that to represent GrIS MB and given the ISSM forcing you have to combine ISSM with MAR v3.5.2 and not MAR v2.0

In response to reviewer #1, we have clarified in Section 2.2 that MAR v2.0 is only used for derivation of parameters used in filtering, while MAR v3.5.2 is used in the comparison with GRACE. We have also added this sentence near the end of Section 2.3:

“The cumulative mass change from MAR v3.5.2 and ISSM are then combined for comparison with GRACE.”

p. 6354

l. 1: “at a high resolution” -> temporal resolution? Spatial resolution? Both?

“High resolution” has been changed to “the spatial and temporal resolution of the GRACE-LM solution”

Last sentence: I don't understand this sentence here. Isn't the job done by MAR and ISSM models? Or may be the sentence should be moved to the beginning of the paragraph as an introduction?

Since the GRACE solution is estimating ice sheet mass change, and hydrological changes over land areas are accounted for during GRACE processing, one might expect that GRACE processing would include removal of changes in snow cover over land. This is not the case, meaning that the GRACE solution also includes mass changes from tundra areas along the margins of the ice sheet. The sentence is

probably more appropriate in the section describing MAR data, so we have moved it to Section 2.2 and have modified it as follows:

“For comparison with GRACE, we include MAR SMB for the entire island of Greenland, including the GrIS, peripheral ice-covered areas, and tundra areas, as Greenland mass changes related to snow and ice cover outside of the ice sheet boundaries are not removed in the GRACE solution.”

p. 6356

l. 2-4: Any reference for the 2000 m elevation limit between positive and negative MB?

The constraint regions are defined by Luthcke et al. (2013). The 2000 m boundary is a rough estimate of the boundary between positive and negative SMB (the equilibrium line altitude) and is not exact. A reference is added for Luthcke et al. (2013).

p. 6357

l. 1: Explain x and μ .

We have clarified the meaning of x and μ :

“...where x is the x -coordinate and μ is the mean of the distribution...”

l. 21-22: It looks to me that this sentence is a repetition of lines 16-18. Is there a physical meaning/interpretation for λ_i ?

We have removed the statement on lines 16-18 at the suggestion of Reviewer #1. We have explained that the leakage parameter “represents the fraction of mass in mascon j outside the constraint region that influences the mass change in mascon i .”

p. 6358

l. 12: explain t_0 .

Time t_0 is not a single point in time, but represents a point in the timeseries for which temporal filtering is conducted. We have clarified that “ t_0 is a point in time along the timeseries” and have noted that “The filtering was applied at each time t_0 to produce a timeseries of filtered cumulative mass change.”

l. 21: “iteratively adjusted” using the least squares method? Also σ_l or l is not explained or present in formulas (same in p. 6359 l. 1). How was the iteration initiated and modifications performed?

“ l ” was a typographical error and σ_l has been changed to σ_i . The procedure was iterative in the sense that we repetitively applied filtering with different combinations of each parameter, but not in the sense that the parameters at a given

point were chosen based on the level of agreement for the previous set of parameters. We simply tried all combinations of the specified range of parameters, and subsequently found the combination of parameters that yielded the minimum RMSE. We have slightly changed and reorganized the text for clarity:

“We iteratively adjusted the values of σ_i , σ_{time} (in the case of temporal filtering), and λ_{ij} , for each mascon i . Values of σ_i were varied at 10 km increments over a range of 1 to 600 km, while values of σ_{time} ranged between 1 and 91 days at increments of 5 days, and λ_{ij} ranged between 0 and 1 at increments of 0.01. We tried all combinations of the three parameters over these ranges. The combination of parameters that yielded the minimum root mean squared error (RMSE) between the Gaussian-filtered and GRACE-LM-filtered cumulative mass timeseries were taken as the optimal set of parameters.”

p. 6359

l. 1 what was the initial values of sigma i, sigma time and lambda i?

σ_i has been changed to σ_i . The range of parameters has been noted in this paragraph. The “initial” value does not matter in the identification of the best combination of parameters, as we simply tried all combinations over the specified set of ranges. The range of parameters was the same for the case where values of σ_i , σ_{time} and λ_i were the same for all mascons. We have modified the sentence for clarity:

“We also tried applying the same values of σ_i , σ_{time} , and λ_{ij} across all mascons i over the specified range of each parameter, but it was found that by spatially varying the values of these parameters the errors were reduced.”

p. 6360

l. 5: You should precise the type of interpolation you use here.

We now note that we used linear interpolation.

l. 6: please explain how you remove the linear trends (least squares adjustment, moving window average...)

For clarity we have modified the text as follows:

“We then subtracted the long-term linear trend for the entire timeseries (2003-2012) obtained from least-squares regression, and averaged the data for a given day of the year across all available years.”

p. 6352

l. 1: Would “Additional temporal Gaussian-filtering improves the agreement between the spatial Gaussian-filtered...” be better ?

Agreed. The text has been modified to read: "Adding temporal Gaussian-filtering..."

p. 6363

Don't you have uncertainties on your trend estimates?

We have calculated uncertainties on the trend estimates and have added these to the text, as well as a description in Section 2.4.4:

"We also compared modeled and GRACE-LM trends for the 2003-2012 period. To calculate the uncertainty in trends from GRACE-LM, we employed a similar procedure to estimate uncertainty in trends, conducting 10,000 Monte Carlo simulations and obtaining a distribution of trends and uncertainty values (from the 95% confidence interval for calculated each trend). The error on the trend was calculated as the average of the 2.5% and 97.5% deviations from the trend added to the 97.5% (upper) bound on the distribution of uncertainty values. For all model estimates, uncertainty on trends is reported as the 95% confidence interval obtained during linear regression."

l. 17: "2000-2012" isn't it "2003-2012"?

Yes, 2003-2012 is correct. The text has been changed.

p.6364

l. 1-3: Consistency -> $-150 - 30 = -180$ Gt/yr different to -179 Gt/yr in l. 14, p. 6363. Same for $-242 + 3 = -239$ Gt/yr w.r.t. -240 Gt/yr.

These errors have now been corrected.

l. 4-end: It looks like only models can be wrong, what about GRACE-LM ? Are you accurately taking all geophysical effects into account?

Errors associated with processing GRACE-LM data are accounted for in the error estimates for the GRACE-LM solution. The GRACE-LM solution produces trends comparable to those of other GRACE solutions, within the range of specified errors for the different solutions (Luthcke et al., 2013). We have added a mention of this in Section 2.1. We have added estimates of uncertainty on the trends and the differences between the filtered model results and GRACE exceeds the uncertainty on the difference. We have noted this in Section 3.1.

p. 6365

l. 7-8. Can you suggest examples for independent evaluations of the models?

We have added some suggestions as follows:

"In these areas, high spatial variability of topography can strongly influence SMB. To properly identify the source of the differences, further independent evaluations of

MAR SMB and ISSM DMB are needed, for example, comparison between ISSM and remote-sensing derived discharge estimates (e.g. Rignot and Kanagaratnam, 2006), or comparison between MAR and additional in situ measurements in ablation areas.”

p. 6368

l. 1: “the maximum modeled mass occurs” -> “the maximum modelled mass CHANGE occurs”?

For clarity we have changed “the maximum modeled mass” to “the maximum in the cycle of cumulative mass change”.

p. 6369

l. 15: Can you give examples of non-ice-sheet-related processes that may contribute to the discrepancy?

See response to the last point in the general comments. We have added the following here:

“Additionally, it is possible that although the GRACE-LM solution includes error estimates associated with the forward models used in GRACE processing, unaccounted for errors, such as errors in model simulations of atmospheric or ocean circulation (for which observations for validation are limited) may contribute to the differences. However, we cannot envision any obvious reason for the discrepancy other than the potential errors in ISSM or MAR v3.5.2 that have been noted.”

l. 17: I would change “Discussion and conclusions” to “Concluding remarks”.

Changed as suggested.

l. 23-25: “We also find that ... this effect.” What about something like “We also applied a temporal Gaussian filter to the models to reproduce the attenuation inherent to the GRACE-LM processing strategy.”?

The sentence has been changed to:

“We have therefore also applied a temporal Gaussian filter to the model outputs to reproduce the attenuation inherent to GRACE-LM processing.”

p. 6370

l. 13-14: How many in situ stations? How many SMB measurements are available?

There are eight stations along the Kangerlussuaq Transect in west Greenland (compared with MAR in Colgan et. al. 2015), there are also a handful of stations from the PROMICE network with stakes in areas of net ablation on the ice sheet (www.promice.org). The sentence has been modified as follows:

“A comparison at eight in situ stations at the Kangerlussuaq transect on the southwest GrIS suggests that MAR v3.5.2 SMB is closer to in situ measurements (Colgan et al., 2015), but such measurements are limited to this transect with the exception of a comparable number of ablation stake locations from the Programme for Monitoring of the Greenland Ice Sheet (PROMICE; www.promice.org).”

l. 19: Any suggestion for conducting independent evaluation of each model?

We have added some suggestions as follows:

“The only means of determining the relative contribution of ISSM and MAR v3.5.2 to underestimated mass loss would be to conduct an independent evaluation of each model against DMB (e.g. using the methods of Rignot and Kanagaratnam, 2006) and SMB estimates over large portions of the GrIS. These analyses are beyond the scope of this study, and the evaluation of SMB is limited by sparsely available data, although radar measurements of snow accumulation may help to fill this gap. A preliminary comparison by Koenig et al. (2015) suggests that there is a good agreement between MAR v3.5.2 and radar-derived accumulation estimates over the interior of the GrIS during the years 2009-2012, but that MAR tends to overestimate accumulation along the southeastern coast.”

l. 27: “represented” -> observed? “results” -> predictions?

“as represented by” has been changed to “from”. “results” has been changed to “outputs”. We feel that “predictions” implies a representation of future behavior, which is not the case for these model outputs.

p. 6372

l. 8: “and may transition between”?

The sentence has been modified for clarity:

“Different glaciers exhibit different patterns of flow variability, and a single glacier may exhibit different patterns of flow in different years.”

fig. 3: RMSD -> RMSE?

RMSD has been changed to RMSE as suggested.

fig. 5 and where it appears: errors bars are not that easy to identify.

We are not sure exactly which error bars the reviewer was referring to. We did not have vertical error bars on the 95% range of the distribution; these have now been added.

fig. 6: can't see the pink shading surrounding the GRACE time series. 2003-2013? Be consistent with the manuscript where it is mentioned 2003-2012.

Fig. 6 has been changed so that the timeseries extends from 2003-2012 for consistency with most of the text. "2012" was changed to "2013" in the caption. The error is small relative to the trend, and pink shading was obscured by the timeseries line. The width of the line has been reduced to allow the pink shading to be more visible.

fig. 9: 2003-2013 or 2003-2012? In b), missing an x in maximum. It would be easier for comparison purpose to have the same colour scale in all figures.

"2013" has been changed to "2012". The typo in "maximum" has been corrected. Most of the time, the dates for the maximum and minimum peaks do not overlap. We have adjusted the color scales so that the same scale is used for images of maximum and minimum peaks.

fig. 10: "and blue colours indicate AND earlier date" -> typo?

Yes, this was a typo. "and" has been changed to "an"

fig. 12b: Could satellite altimetry data help assessing the difference between models and GRACE data?

Previous studies have focused on annual trends rather than seasonal trends, as the temporal resolution of altimetry data are limited. The historical altimetry measurements available for the period used in our study will likely not help to assess the differences shown in Figure 12. However, newly launched sensors, such as Cryosat-2 and Sentinel3 might provide higher temporal resolution and we appreciate the suggestion by the reviewer in this regard. Still, translating elevation changes into mass changes is still strongly dependent on the firn compaction models adopted and a more detailed, long-term study is required in this regard.

Greenland Ice Sheet seasonal and spatial mass variability from model simulations and GRACE (2003-2012)

P. M. Alexander^{1,2,3}, M. Tedesco^{2,1,4}, N-J. Schlegel^{5,6}, S. B. Luthcke⁷, X. Fettweis⁸, and E. Larour⁶

[1]{Graduate Center of the City University of New York, 365 5th Ave., New York, NY, 10016 USA}

[2]{City College of New York, City University of New York, 160 Convent Ave., New York, NY, 10031 USA}

[3]{NASA Goddard Institute for Space Studies, 2880 Broadway, New York, NY, 10025, USA}

[4] {Lamont Doherty Earth Observatory, Columbia University, 61 Route 9W, Palisades, NY, 10964, USA}

[5]{Joint Institute for Regional Earth System Science and Engineering, University of California, Los Angeles, CA, 90095 USA}

[6]{Jet Propulsion Laboratory, California Institute of Technology, 4800 Oak Grove Drive MS 300-227, Pasadena, CA, 91109 USA}

[7]{Planetary Geodynamics Laboratory, NASA Goddard Space Flight Center, Greenbelt, MD 20771, USA}

[8]{Laboratory of Climatology, Department of Geography, University of Liège, n°2 Allé du 6 Aout, 4000, Liège, Belgium}

Correspondence to: P. M. Alexander (patrick.m.alexander@nasa.gov)

Abstract

Improving the ability of regional climate models (RCMs) and ice sheet models (ISMs) to simulate spatiotemporal variations in the mass of the Greenland Ice Sheet (GrIS) is crucial for prediction of future sea level rise. While several studies have examined recent trends in GrIS mass loss, studies focusing on mass variations at sub-annual and sub-basin-wide scales are

still lacking. At these scales, processes responsible for mass change are less well understood and modeled, and could potentially play an important role in future GrIS mass change. Here, we examine spatiotemporal variations in mass over the GrIS derived from the Gravity Recovery and Climate Experiment (GRACE) satellites for the January 2003 – December 3– 2012 period using a “mascon” approach, with a nominal spatial resolution of 100 km, and a temporal resolution of 10 days. We compare GRACE-estimated mass variations against those simulated by the Modèle Atmosphérique Régionale (MAR) RCM and the Ice Sheet System Model (ISSM). In order to properly compare spatial and temporal variations in GrIS mass from GRACE with model outputs, we find it necessary to spatially and temporally filter model results to reproduce leakage of mass inherent in the GRACE solution. Both modeled and satellite-derived results point to a decline (of -178.9 ± 4.49 and -239.4 ± 7.740 Gt yr⁻¹ respectively) in GrIS mass over the period examined, but the models appear to underestimate the rate of mass loss, especially in areas below 2000 m in elevation, where the majority of recent GrIS mass loss is occurring. On an ice-sheet wide scale, the timing of the modeled seasonal cycle of cumulative mass (driven by summer mass loss) agrees with the GRACE-derived seasonal cycle, within limits of uncertainty from the GRACE solution. However, on sub-ice-sheet-wide scales, there are significant differences in the timing of peaks in the annual cycle of mass change. At these scales, model biases, or unaccounted-for processes related to ice dynamics or hydrology may lead to the observed differences. This highlights the need for further evaluation of modelled processes at regional and seasonal scales, and further study of ice sheet processes not accounted for, such as the role of sub-glacial hydrology in variations in glacial flow.

1 Introduction

The Earth’s ice sheets represent substantial reservoirs of water stored in the form of ice, which contribute to fluctuations in global sea level. The Greenland Ice Sheet (GrIS) in particular is estimated to have lost mass at an average rate of -142 ± 49 Gt yr⁻¹ between 1992 and 2011 (Shepherd et al., 2012). Roughly 50% of recent GrIS mass loss is associated with surface mass loss (Rignot et al., 2011; van den Broeke et al., 2009), characterized by multiple records in GrIS melt extent and duration over the past decade (Tedesco et al., 2008, 2011, 2013a; Nghiem et al., 2012) which has led to increased meltwater runoff that exceeds small increases in ice-sheet-wide precipitation (van den Broeke et al., 2009; Ettema et al., 2009;

Fettweis et al., 2013a). The other portion of GrIS mass loss is associated with an acceleration of outlet glaciers (Rignot et al., 2011). The speedup of glaciers has been attributed to warming oceans (Rignot et al., 2012) and lubrication of the GrIS bed from meltwater generated at the surface, and channeled from the surface to the bed by vertical conduits, allowing glaciers to slide more easily (Zwally et al., 2002). This second factor has been shown to be more complex than initially thought, resulting in speed-ups or slow-downs that depend on the volume of meltwater reaching the bed and the time of year (e.g. Sundal et al., 2011).

Previous studies have generally focused on decadal trends in GrIS mass and the ability of models to capture these trends (e.g. Shepherd et al., 2012; Rignot et al., 2011), but seasonal variations in mass, and spatial variations at sub-basin-wide scales have not been explored extensively. At smaller temporal and spatial scales, poorly understood processes may play a particularly important role in mass variability. For example, numerous studies have identified seasonal variations in glacial flow (Bartholomew et al., 2010; Howat et al., 2010; Joughin et al., 2008, 2014; Moon et al., 2014), and local variations in flow associated with lake drainage events or summer melting (Das et al., 2008; Tedesco et al., 2013b; Hoffman et al., 2011). Ice sheet hydrology can also contribute to local variations in mass. For example, an observational study by Rennermalm et al. (2013) suggests that within one catchment along the GrIS coast, up to 50% of runoff generated at the surface may have been stored within the ice sheet over multiple seasons. Water can also be stored at or near the surface of the ice sheet, within supraglacial lakes, or within firn aquifers, which were recently discovered to persist during winter over large areas of the southwest and southeast GrIS margins (Forster et al., 2013; Koenig et al., 2014). While the amount of water stored within supraglacial lakes is likely small relative to the overall rate of GrIS mass change-MB (Smith et al., 2015), the amount of water stored within the firn aquifers or englacially is currently unknown.

The overall GrIS mass balance (MB), the rate of ice sheet mass change, is generally considered to consist of two components, the Surface Mass Balance (SMB, i.e. the balance between accumulation and ablation at the ice sheet surface), and ice discharge (D), such that $MB = SMB - D$. Simulations of SMB at high spatial and temporal resolutions (e.g. daily temporal resolution and <25 km spatial resolution) are conducted by Regional Climate Models (RCMs; e.g. Fettweis et al., 2013a; Ettema et al., 2009), and D can be simulated by Ice Sheet Models (ISMs) (e.g. Larour et al., 2012; Quiquet et al., 2012; Robinson et al., 2011;

Huybrechts et al., 2011), which simulate glacial flow subject to SMB forcing. At seasonal and sub-basin-wide scales other processes become more important, so that the full mass balance is expressed as follows (after Cuffey and Paterson, 2011):

$$MB = SMB + EMB + BMB + DMB \quad (1)$$

where EMB is the englacial mass balance, BMB is the basal mass balance, and DMB is the mass balance associated with dynamic flow. Most processes related to EMB or BMB, as well as variations in DMB associated with ice-ocean interactions and meltwater lubrication are not accounted for by either RCMs or ISMs. In a warmer climate, more meltwater production and runoff is expected (Fettweis et al., 2013b), suggesting that unaccounted for processes will play an increasingly important role in future GrIS mass balance (Chu, 2014), and should be included in model projections of mass change.

Cognizant of the potential role of such processes in GrIS MB, and the need for evaluation of the combined results of ISMs and RCMs, we conducted a comparison between satellite-derived mass changes from the Gravity Recovery and Climate Experiment (GRACE; Luthcke et al., 2013), modeled DMB from the Ice Sheet System Model (ISSM; Larour et al., 2012), and SMB from the Modèle Atmosphérique Régionale (MAR; e.g. Fettweis et al., 2013a) for the period January 2003 through December -2012. The GRACE solution of Luthcke et al. (2013) (hereafter referred to as GRACE-LM) is provided at a high spatial and temporal resolution compared to other GRACE solutions (~100 km and 10 days respectively). We aggregate model results to the GRACE-LM grid and spatially and temporally filter the aggregated outputs in order to match inherent spatial and temporal attenuation of the GRACE-LM product (as discussed by Luthcke et al., 2013; Sabaka et al., 2010). After filtering model outputs, we compared spatial patterns of simulated and satellite-derived mean annual mass balance, the mean annual cycle of mass change, and the spatial distribution of the timing of the seasonal cycle. This analysis has two purposes: (1) to evaluate seasonal and spatial variations in mass from the combined results of an RCM and ISM applied over the GrIS, and (2) to reveal and analyse any discrepancy between GRACE-derived and simulated mass changes not accounted for by the simulationsmodeled mass changes, while accounting for uncertainties associated with the GRACE-LM solution.

2 Data and Methods

2.1 GRACE data

We used the iterated global GRACE solution of Luthcke et al. (2013), which utilizes a mass concentration (mascon) approach to derive spatially and temporally distributed changes in the mass of land ice, at a 1 arc-degree (~100 km) spatial resolution and 10-day temporal resolution. The solution is available for the period January 2003 through June 2013, but we focus on the January 2003 through December 2012 period to avoid including an incomplete year in our analysis. GRACE-LM mass change estimates are provided for ~100x100 km² “mascon” regions, on what is essentially an equal area grid (shown in Fig. 1a). All GRACE solutions are ultimately derived from k-band range and range rate (KBRR) data for two co-orbiting satellites roughly 220 km apart (Tapley et al., 2004). The Luthcke et al. (2013) solution, used in this study, differs from other solutions in its approach: models of satellite motion are used to compute KBRR from forward-modeled mass changes, and through iteration, the residuals between the computed and observed KBRR are minimized. This contrasts with the spherical harmonic approach (e.g. Velicogna and Wahr, 2006) in which a set of Stokes coefficients or spherical harmonic fields provided by GRACE processing centers are spatially filtered and used to estimate spatial and temporal variations in mass. The mascon approach of Luthcke et al. (2013) attempts to minimize the loss of signal associated with processing GRACE data, and detailed error estimates, accounting for various steps in processing, are provided. The Luthcke et al. (2013) solution agrees within error estimates with other estimates for GrIS mass change derived from GRACE. As described by Luthcke et al. (2013), forward modelling is used during the processing of GRACE data to isolate the signal associated with land-ice changes. In particular, the static gravity field, orbital parameters, ocean and earth tides, terrestrial water storage, variations in mass associated with atmospheric and ocean circulation, and glacial isostatic adjustment are simulated by various models, and these simulated changes are used to correct GRACE-estimated mass change. The errors associated with each of these simulations are included in calculations of error for each GRACE-LM mascon. The GRACE-LM mascons are distributed at a resolution that is higher than the fundamental spatial resolution of GRACE (Luthcke et al., 2006), so that there is “leakage” of mass into and out of each mascon. This results in a spatial “smoothing” effect such that the change in mass for the area represented by a mascon is distributed over a radius of roughly 600 km from the mascon center (Luthcke et al., 2013). As a result, model outputs

need to be consistently spatially filtered to allow a fair comparison with the GRACE-LM data. The details of this process are described further in Section 2.4.

2.2 The MAR RCM

The MAR RCM (Gallée and Schayes, 1994; Gallée, 1997; Lefebvre et al., 2003) is a coupled surface-atmosphere RCM that has been applied over the GrIS to simulate current and future changes in SMB (e.g. Fettweis et al., 2013a; Franco et al., 2013). The atmospheric portion of MAR is described by Gallée and Schayes (1994), while the land surface model is the Soil Ice Snow Vegetation Atmosphere Transfer scheme (SISVAT), containing the Crocus snow model (Brun et al., 1992). We use model outputs from two versions of the MAR model, MAR v2.0 (used by Fettweis et al., 2013a) for the period January 2003 – December -2010, with the model domain and setup described by Fettweis (2007), and MAR v3.5.2, the latest version of MAR (used by Colgan et al., 2015), for the period January 2003 – December -2012. For comparison with GRACE, we include MAR SMB for the entire island of Greenland, including the GrIS, peripheral ice-covered areas, and tundra areas, as Greenland mass changes related to snow and ice cover outside of the ice sheet boundaries are not removed in the GRACE solution. An overestimation of accumulation simulated by MAR v2.0 in the interior of the ice sheet (Vernon et al., 2012) was in part corrected in MAR v3.5.2 by slightly increasing the snowfall rate, producing more precipitation along the ice sheet margin and less inland. According to the recommendations of Alexander et al. (2014), MAR v3.5.2 features an updated bare ice albedo exponentially varying between 0.4 (dirty ice) and 0.575 (clean ice) as a function of the accumulated surface water height and slope. The bare ice albedo was fixed at 0.45 in MAR v2.0. Both MAR v3.5.2 and MAR v2.0 are forced every 6 hours at the lateral boundaries by the ERA-Interim reanalysis (Dee et al., 2011) beginning in January 1979, and are run at a 25 km spatial resolution (as shown in Fig. 1b). This paper primarily focuses on results from MAR v3.5.2, which is used to force the ISSM ice sheet model. As will be discussed further in Section 2.4.2, the computationally intensive processing used in processing of GRACE-LM outputs had previously been applied to MAR v2.0 outputs, and we used these filtered MAR v2.0 outputs for the purpose of deriving a spatial filter to approximate spatial attenuation in the GRACE-LM solution.

2.3 The ISSM Model

ISSM (Larour et al., 2012) is a thermo-mechanical ice sheet model that simulates ice flow in response to forcing from surface mass balance. The model solves equations for conservation of mass, momentum, and energy, in conjunction with constitutive equations for ice properties and boundary conditions. It has the capability of incorporating multiple approximations to the full-Stokes (FS) ice flow equations in different regions. The model is implemented on a finite element mesh, which can be refined anisotropically to allow for a higher resolution in areas of high gradients in observed surface velocities. Inversion methods are used to derive constitutive properties such as ice rigidity and basal friction, by iteratively minimizing differences between radar-derived observed and modeled ice velocities (Morlighem et al., 2010; Larour et al., 2012).

In this study, ISSM has been run over the entire GrIS, following the model configuration of Schlegel et al. (2015), which uses a 2D Shelfy-Stream Approximation (~~SSA~~) to the FS equations (MacAyeal, 1989) in order to increase computational efficiency (as described by Larour et al., 2012). Aside from the inversion methods used to perform initialization of parameters for ice properties and basal friction, the model is forced only by SMB at the surface, subject to the boundary conditions described by Larour et al. (2012). Bedrock topography is defined using the radar and mass-conservation-derived dataset of Morlighem et al. (2015) (described in Morlighem et al., 2014). The GrIS simulation consists of an anisotropic mesh, which ranges in spatial resolution from 1 km to 15 km, consisting of 91,490 elements. The MAR v3.5.2 mean SMB for the period January 1979 – December -1988 is interpolated to a 5 km resolution using the method of Franco et al. (2012) to correct SMB with respect to subgrid topography as a function of the local vertical gradient of SMB, and is subsequently interpolated onto the ISSM mesh. Then it is used to spin up ISSM until the model reaches steady-state equilibrium, i.e. the change in GrIS mass over time is negligible (as described by Schlegel et al., 2013). Once the model reaches steady-state (after 30,000 years in this case), ISSM is forced monthly with SMB from the climate reconstruction of Box et al. (2013) and Box (2013) for the period January 1841 – December -1979, adjusted so that the mean SMB for this period is equal to the MAR mean SMB of January 1979 – December -1988. This ensures that ISSM responds to mean SMB from MAR, but incorporates anomalies from this mean beginning in 1841. MAR v3.5.2 SMB for the period January -1979 – December -2013 is then used to force ISSM at a daily temporal resolution with a model

timestep of 12 hours. The cumulative mass change from MAR v3.5.2 and ISSM are then combined for comparison with GRACE. ~~We evaluate the ISSM spin-up by comparing the ISSM ice thickness at steady state to the ice thickness obtained from the mass conservation dataset of Morlighem et al. (2015), derived from radar data for 1993–2014, interpolated onto the ISSM mesh. We also compare ISSM annual ice velocities with the radar-derived ice velocity data of Rignot and Mouginot (2012), derived from data spanning 2008–2009.~~ ISSM mean DMB for the period January 2003 – December 2012 is shown in Fig. 1c.

2.4 Methods of Comparison

In order to properly compare model results with the GRACE-LM solution, it was necessary to first spatially aggregate model data to the GRACE grid, to account for the different resolution of different products (Sect. 2.4.1). Second, in order to conduct a fair comparison with GRACE-LM at the spatial and temporal resolution of the GRACE-LM solution ~~a high resolution~~, model results must be spatially and temporally filtered to account for spatial and temporal attenuation of the GRACE signal, associated with the “leakage” of mass changes from each mascon into nearby mascons in space and time (Luthcke et al., 2013). The best means of filtering model data for comparison to GRACE-LM is to apply the equations used in GRACE-LM processing directly to the model data (Sect. 2.4.2). Because this process is computationally intensive, however, we approximated the effect of GRACE-LM processing using spatial and temporal Gaussian filters (Sect. 2.4.3). Although our approximation does not perfectly reproduce the effect of GRACE filtering in space and time (Sect. 2.4.5), we adopt a statistically conservative approach in our comparison between GRACE-LM and model outputs, to identify cases where differences are unlikely to be a result of filtering or errors in the GRACE-LM solution (discussed in Sect. 2.4.4).

2.4.1 Spatial aggregation

MAR and ISSM daily outputs for the period January 2003 – December 2012 were spatially aggregated into GRACE-LM mascons (Figs 1d and 1e). In the case of ISSM data, ISSM dynamic thickness changes (ice thickness change associated only with dynamic motion of ice) on the anisotropic mesh were first interpolated onto a 10 km equal area grid, converted into mass changes using the density of ice (917 kg m^{-3}) and then aggregated to the nearest GRACE-LM mascon to produce timeseries of DMB for each mascon. In the case of MAR data, MAR SMB outputs at a 25 km resolution were aggregated to the nearest mascon. The

sum of mass change simulated by each model was then calculated for each mascon. Over the oceans, all mass changes predicted by MAR (likely associated with accumulation over sea ice) were set to zero, as such accumulation does not result in changes in mass due to the presence of isostatic adjustment of sea ice over the oceans. ~~MAR SMB over non-glaciated land areas was included when aggregating MAR data into mascons. Snow accumulation and melt over GrIS land areas are not corrected for in GRACE-LM data, and therefore must be included in the comparison.~~

2.4.2 Spatial and temporal filtering using GRACE equations

The GRACE-LM solution uses a Gauss-Newton (GN) procedure to adjust an equivalent height of water within each mascon to produce perturbations in the GRACE spherical harmonic fields or Stokes coefficients. The partial derivatives of the Stokes coefficients with respect to the equivalent water height, and the partial derivatives of KBRR with respect to the Stokes coefficients are then used to determine the change in KBRR associated with a change in equivalent water height. The GN procedure iteratively adjusts equivalent water height within all mascons to minimize the residuals between computed KBRR and KBRR observations. The final GRACE-LM solution for a given mascon is not the “true” mascon state, but differs from it due to “leakage” between mascons and the presence of noise in the solution. The relationship between the true mascon state h_k and the updated mascon state \tilde{h}_k is given by Equation 8 of Luthcke et al. (2013), expressed as :

$$\tilde{h}_{k+1} = Rh_k + Ke \quad (2)$$

where e represents added noise, and R is referred to as the resolution operator, as it serves the function of “smoothing” the true mascon states h_k in space and time. K and R are in turn expressed by:

$$K = (L^T A^T W A L + \mu P_{hh})^{-1} L^T A^T W \quad (3)$$

$$R = K A L \quad (4)$$

where L represents the partial derivatives of the Stokes coefficients with respect to the mascon state, A represents the partial derivatives of the KBRR observations with respect to the Stokes coefficients, and W is a data weight matrix that accounts for orbital parameters and corrections for processes not related to ice sheet mass changes (e.g. isostatic adjustments, tides, etc.). P_{hh} is a regularization matrix, which constrains the solution so that differences in

mass change between mascons closer together are minimized (Sabaka et al., 2010). Constraint regions for the GrIS are also defined (Fig. 1a) such that the constraint does not apply across the boundaries of the constraint region. Thus, for the GrIS, changes in mass above 2000 m in elevation, where the MB is generally positive, can occur independently of changes in mass below 2000 m in the GRACE-LM solution (Luthcke et al., 2013).

In order to spatially filter MAR data to match GRACE-LM, we applied the resolution matrix to the aggregated MAR v2.0 data, using Equation 2, taking the aggregated MAR v2.0 on GRACE-LM mascons as the “true” mascon states h_k , and ignoring the added noise term e .

The resulting updated mascon states \tilde{h}_{k+1} are MAR v2.0 data spatially and temporally filtered to match GRACE-LM. The effect of spatial smoothing on the MAR v2.0 aggregated outputs (Fig. 2a), along with the impact of different constraint regions above and below 2000 m in elevation, can be seen in Fig. 2b, which shows the mean January 2003 – December 2010 MAR v2.0 outputs filtered using the resolution matrix. As expected, the spatial filtering decreases the magnitude of mass change for individual mascons by redistributing mass change across other surrounding mascons.

Unfortunately, the methods discussed above (hereafter referred to as “GRACE-LM filtering”) are computationally expensive and time consuming to perform. We only applied GRACE-LM filtering to MAR v2.0 outputs as only these outputs were available when the GRACE-LM filtering procedure was applied. To filter MAR v3.5.2 and ISSM data, we employed an approximation to the GRACE-LM filtering procedure, which is described further below.

2.4.3 A Gaussian approximation to GRACE-LM filtering

As discussed by Luthcke et al. (2013), the leakage associated with individual GRACE-LM mascons is roughly equivalent to a spatial Gaussian filter with a radius of 300 km, with the mascons within a 600 km radius accounting for almost 100% of the mass changes within a mascon. To allow for spatial filtering of MAR v3.5.2 and ISSM outputs, we developed an approximation to the GRACE-LM filtering using a Gaussian filter. The Gaussian function can be expressed as a function of distance from the center of the distribution $(x-\mu)$, where x is the x -coordinate and μ is the mean of the distribution, and a standard deviation (σ) as:

$$g(x) = \frac{1}{\sigma\sqrt{2\pi}} e^{-\frac{1}{2}\left(\frac{x-\mu}{\sigma}\right)^2} \quad (5)$$

We used a gaussian function to weight the data for all surrounding mascons (j) as a function of radial distance from a central mascon (i). In this case, $x-\mu$ is replaced by the distance from a central location to another mascon (r_{ij}), and a discrete approximation to the Gaussian is used, as follows:

$$g(r_{ij}) = e^{-\frac{1}{2}\left(\frac{r_{ij}}{\sigma_i}\right)^2} \quad (6)$$

$$w_j = \frac{g(r_{ij})}{\sum_{j=1}^n g(r_{ij})} \quad (7)$$

The weight, w_j , assigned to a given mascon, j , at a distance r_{ij} from mascon i , is given by the value of the Gaussian function at the center of mascon j divided by the sum of all Gaussian values surrounding mascon i . A different σ_i value is chosen for each mascon, as will be explained further below.-

We further modify Eq. (7) to account for the constraint regions discussed in the previous section, which for the GrIS, includes areas above and below 2000 m in elevation (Luthcke et al., 2013). For a given mascon within a constraint region (mascon i), weights for mascons outside of the constraint region were multiplied by a leakage parameter, λ_{ij} , which represents the fraction of mass in mascon j outside the constraint region that influences the mass change in mascon i which was set to 1 within the constraint region, and a fixed value between 0 and 1 outside of the constraint region.- Accounting for these constraints, Eq. (7) becomes:

$$w_j = \frac{g(r_{ij})\lambda_{ij}}{\sum_{j=1}^n g(r_{ij})\lambda_{ij}} \quad (8)$$

Where λ_{ij} for mascon i is set equal to 1 within the constraint region, and equal to a constant value between 0 and 1 for all mascons j outside of the constraint region.

The weights for mascons j surrounding a central mascon i are then used to create a weighted average of mass change for mascon i ($\Delta m_{i,new}$) as a function of the modeled changes for mascon i (Δm_i) and mascons j (Δm_j):

$$\Delta m_{i,new} = \Delta m_i w_i + \sum_{j=1}^n \Delta m_j w_j \quad (9)$$

Finally, we added a time component to the filtering procedure, as the regularization matrix (P_{hh}) discussed in Section 2.4.2 also includes a temporal component (Sabaka et al., 2010), and because GRACE-LM-filtering alters both the amplitude and timing of the seasonal cycle of mass change (as discussed in Section 2.4.5). After applying the spatial filter described by Eqs. (6) and (8), timeseries of cumulative mass from MAR v2.0 were interpolated onto GRACE-LM time-intervals. We then applied a temporal Gaussian filter to the cumulative mass timeseries for each mascon, using the temporal radius $\Delta t_{t_0 t_k}$, where t_0 is a point in time along the timeseries, t_k is a time before or after the time t_0 , and $\Delta t_{t_0 t_k} = |t_k - t_0|$:

$$g(\Delta t_{t_0 t_k}) = e^{-\frac{1}{2} \left(\frac{\Delta t_{t_0 t_k}}{\sigma_{time}} \right)^2} \quad (10)$$

$$w_{ik} = \frac{g(\Delta t_{t_0 t_k})}{\sum_{k=n}^m g(\Delta t_{t_0 t_k})} \quad (11)$$

where n is the first value in the timeseries being filtered and m is the last value. The filtering was applied at each time t_0 to produce a timeseries of filtered cumulative mass change.

We applied the spatial and temporal filters discussed above to the aggregated unfiltered MAR v2.0 data, and compared the resulting cumulative mass timeseries' from each mascon to the GRACE-LM filtered MAR v2.0 timeseries. Two filtering procedures were employed, one in which only spatial filtering was performed, and another in which both spatial and temporal filtering were performed to determine the impact of temporal filtering. We ~~iteratively~~ iteratively adjusted the values of σ_i , σ_{time} (in the case of temporal filtering), and λ_{ij} , for each mascon i . Values of σ_i were varied at 10 km increments over a range of 1 to 600 km, while values of σ_{time} ranged between 1 and 91 days at increments of 5 days, and λ_{ij} ranged between 0 and 1 at increments of 0.01. ~~The~~ We tried all combinations of the three parameters over these ranges. The combination of parameters that yielded the minimum root mean squared error (RMSE) between the Gaussian-filtered and GRACE-LM-filtered cumulative mass timeseries were taken as the optimal set of parameters for a given mascon. ~~Initially, the~~ We also tried applying the same values of σ_i , σ_{time} , and λ_{ij} ~~were used across for~~ all mascons i , over the specified range of each parameter, but it was found that by spatially varying the values of these parameters the errors were reduced. We also set λ_{ij} equal to zero outside of the island of Greenland as defined by the GRACE-LM mascons, as this improved the agreement with the GRACE-LM-filtered results. ~~Values of σ_i were varied at 10 km increments over a range of~~

~~1 to 600 km, while values of σ_{time} ranged between 1 and 91 days at increments of 5 days, and λ_{ij} ranged between 0 and 1 at increments of 0.01.~~ We tried larger values of σ_i beyond the indicated range at larger increments, but did not find a reduction in RMSE for values larger than 600 km.

Average Gaussian-filtered MAR v2.0 SMB (with both spatial and temporal filtering applied) for the period 2003-2010 is shown in Fig. 2c. The Gaussian-filtered MAR v2.0 SMB is similar to GRACE-LM-filtered SMB. Differences between the GRACE-LM-filtered and Gaussian-filtered results (Fig. 2d) are an order of magnitude smaller than the average SMB values (ranging from -0.2 to 0.2 vs. -2 to 5 Gt), although in some regions where trends in SMB are small, the differences are a large percentage of the average SMB. Optimal values for σ_i , σ_{time} , and λ_{ij} and the RMSE for the Gaussian vs. the GRACE-LM-filtered MAR v2.0 data are shown in Fig. 3. Further discussion of the impacts of filtering on model outputs is provided in Section 2.4.5.

2.4.4 Application of Gaussian filters, ~~and seasonal cycle analysis~~ and trends

Following the choice of the optimal Gaussian filter using MAR v2.0, we applied the same chosen filter to MAR v3.5.2 and ISSM data forced by MAR v3.5.2, aggregated to the GRACE-LM grid. MAR v3.5.2 exhibits a less negative SMB along the Greenland coast and GrIS margins and a less positive SMB within the GrIS interior (Fig. S1) compared with MAR v2.0 (as there is more coastal accumulation and less interior accumulation in MAR v3.5.2). These differences do not affect our ability to filter MAR v3.5.2 outputs, as the Gaussian ~~filtering procedure~~ does not incorporate changes in mass depend on mass changes, but approximates the GRACE-LM resolution operator, which serves to redistribute mass changes subject to specified constraint regions. Spatial filtering of MAR v3.5.2 and ISSM was conducted first at a daily temporal resolution. Filtered cumulative mass timeseries for each mascon were then interpolated onto GRACE-LM time steps, and temporal filtering was performed. We then summed the timeseries of cumulative mass change from MAR v3.5.2 and ISSM, to generate timeseries of integrated MB.

We examined differences between the modeled and GRACE-LM seasonal cycles of cumulative mass change by first linearly interpolating filtered cumulative model and GRACE-LM timeseries ~~to a daily temporal resolution onto daily timesteps.~~ This was necessary because the GRACE-LM timesteps are not evenly spaced, and do not occur at the

1 ~~same point in time every year. We then subtracted, removing linear trends from the long-term~~
2 ~~linear trend for the entire timeseries (2003-2012) obtained from least-squares regression, to~~
3 ~~remove the impact of differences in trends on the timing of the seasonal cycle. After~~
4 ~~removing trends, the timeseries, and averaging the data the cumulative mass value for a given~~
5 ~~day of the year was averaged across all years in the 2003-2012 period, to yield an average~~
6 ~~annual cycle for all years available years. — This was performed for the GrIS-wide timeseries,~~
7 ~~as well as for individual mascons and GrIS sub-regions. — The maximum and minimum peaks~~
8 ~~were computed from this average annual cycle. This was performed for the GrIS-wide~~
9 ~~timeseries, as well as for individual mascons and GrIS sub-regions. — A two-year composite~~
10 ~~seasonal cycle was constructed for GRACE-LM and model data, and the timing of the highest~~
11 ~~local maximum and lowest local minimum in this cycle were identified.~~

12 GRACE data from Luthcke et al. (2013) include estimates of the error associated with the
13 timeseries of cumulative mass change for each mascon. When examining aggregated data, we
14 summed the error for all mascons. The error for a given day for the GRACE-LM seasonal
15 cycle was determined to be the total GRACE-LM error for the cumulative timeseries divided
16 by $\sqrt{n} \sqrt{n}$, where n was the number of years being averaged. Errors in the GRACE-LM
17 timeseries can lead to errors in the timing of the seasonal cycle because random errors can
18 cause a shift in the timing of a local maximum or minimum point. To account for these
19 errors, we performed 10,000 Monte Carlo simulations with the GRACE-LM seasonal data,
20 assuming that the errors in the timeseries were normally distributed. For each of these
21 simulations, we identified the local maximum and minimum peaks in the seasonal cycle,
22 allowing us to generate a distribution of dates for maximum and minimum peaks. ~~The~~
23 ~~temporal resolution of the GRACE-LM dataset can also lead to errors of roughly ± 10 days for~~
24 ~~the timing of any estimate. Because the GRACE-LM timesteps are not regular, the~~
25 ~~uncertainty on the timing of peaks for the average seasonal cycle due to temporal resolution is~~
26 ~~generally smaller than 10 days. Given that the error could be as large as 10 days, however,~~
27 ~~we calculated our error on the timing of seasonal cycle peaks as the 95% confidence interval~~
28 ~~from the Monte Carlo simulations. — If the model peaks fell outside of the 95% confidence~~
29 ~~interval ± 10 days. for this distribution. If model peaks fell outside of this error range, the~~
30 ~~timing of the GRACE-LM and model peaks was deemed to differ.~~

31 ~~We also compared modeled and GRACE-LM trends for the 2003-2012 period. To calculate~~
32 ~~the uncertainty in trends from GRACE-LM, we employed a similar procedure to estimate~~

uncertainty in trends, conducting 10,000 Monte Carlo simulations and obtaining a distribution of trends and uncertainty values (from the 95% confidence interval for calculated each trend). The error on the trend was calculated as the average of the 2.5% and 97.5% deviations from the trend added to the 97.5% (upper) bound on the distribution of uncertainty values. For all model estimates, uncertainty on trends is reported as the 95% confidence interval obtained during linear regression.

2.4.5 Effect of filtering on seasonal variations in mass

As we were interested in examining seasonal variations in mass, we examined the impact of GRACE-LM filtering vs. Gaussian filtering (spatial only and spatial + temporal) on the cumulative timeseries of GrIS-wide mass changes, in relation to the seasonal cycle of mass change from GRACE-LM. While it is not possible to compare GRACE-derived mass changes directly to MAR, given that GRACE also records the effects of changes in DMB, a comparison of de-trended timeseries of cumulative mass can be performed, if it is assumed that seasonal variations in ice discharge are small relative to those of SMB. A qualitative comparison of de-trended unfiltered and filtered MAR v2.0 and GRACE-LM cumulative mass timeseries for the GrIS over January 2003 – December -2010 (Fig. 4), suggests that this is a reasonable first-order assumption for the entire GrIS. (As will be seen in Section 3.2, modeled ice-sheet wide seasonal variability from ISSM is also less than 10% of variability from MAR.) Fluctuations in mass, coinciding with net loss of mass during summer months, and net gain of mass during winter months, are captured by both GRACE-LM and MAR v2.0. The average seasonal cycle of cumulative mass change in Fig. 5a indicates a larger amplitude of mass fluctuations for unfiltered and spatially Gaussian-filtered MAR v2.0 results (of 524 and 500 Gt respectively) relative to GRACE-LM (287 ± 30 Gt), and a closer agreement between the amplitudes of GRACE-LM-filtered MAR v2.0 data (339 Gt) and GRACE-LM. On average, during periods of net ablation, GRACE-LM begins losing mass earlier (by 25 days), and starts gaining mass later (by 8 days) as compared with MAR v2.0 unfiltered data (Table 1). GRACE-LM-filtering changes the timing of the start of mass loss such that the period of simulated mass loss begins 10 days sooner, extending the length of the mass loss period.

When both spatial and temporal Gaussian filtering are applied to the MAR v2.0 data, the amplitude of the seasonal cycle is reduced (to 351 Gt), resulting in a better agreement with GRACE-LM and with the GRACE-LM-filtered MAR v2.0 data (Fig. 5a). The timing of

peaks in maximum and minimum mass are also changed, with the temporally Gaussian-filtered MAR v2.0 data exhibiting an extended period of mass loss (145 days) relative to that of the GRACE-LM-filtered MAR v2.0 data (123 days), resulting in the filtered seasonal cycle peaks occurring within 5 days of GRACE-LM peaks. In all cases, however, the timing of peak mass loss from MAR v2.0 falls within the 95% confidence bounds on maximum and minimum dates for GRACE-LM.

Adding temporal Gaussian-filtering improves the agreement between the Gaussian-filtered MAR v2.0 timeseries and the GRACE-LM-filtered timeseries in terms of amplitude, and lengthens the period of net ablation (perhaps too much relative to the period for GRACE-LM-filtered data). For both methods of Gaussian filtering, the timing of the peaks for filtered MAR v2.0 data fall within the 95% confidence bounds on the timing of the GRACE-LM seasonal cycle.

The comparison of GRACE and MAR timeseries and seasonal cycles in the case of MAR v3.5.2 (Figs. S2 and 5b respectively) is similar to that for MAR v2.0. MAR v3.5.2 features a seasonal cycle of smaller amplitude, likely as a result of snow falling more frequently along the coast, where it is more likely to be balanced by ablation during periods of net accumulation, and where it mitigates ablation during periods of net mass loss. The Gaussian filtering has a similar effect on the MAR v3.5.2 outputs, which are similar in timing to MAR v2.0 outputs (Table 1), by reducing the amplitude of seasonal variability and extending the length of the ablation season to be similar to that of GRACE-LM (Fig. 5b and Table 1). In our analysis of ISSM and MAR v3.5.2 outputs, we have chosen to focus on results obtained with temporal Gaussian filtering applied, as it results in reduced errors relative to the GRACE-LM filtering method. We consider this to be a statistically conservative approach. Because we are not able to fully capture the effect of filtering on the timing of the seasonal cycle, we choose the filter that brings the timing of the seasonal cycle closer to that of GRACE-LM. Thus, in locations where the timing of the Gaussian-filtered cycle falls outside of the range of dates from GRACE-LM, it is very likely that there is a difference between the modeled and GRACE-LM seasonal cycles that is not associated with filtering. In locations where the timing of the Gaussian-filtered cycle falls within the range of dates from GRACE-LM, we cannot confirm a difference.

3 Results

3.1 Trends and spatial differences in modelled vs. measured mean MB

We first examine the timeseries of GrIS cumulative mass as simulated by MAR v3.5.2, ISSM, and GRACE-LM over the 2003-2012 period, as shown in Fig. 6. MAR v3.5.2 cumulative SMB shows a net accumulation of mass over Greenland (of 246.9 ± 4.77 Gt yr⁻¹), which varies seasonally in response to cycles of melting and accumulation. ISSM exhibits a net loss of mass (-425.8 ± 0.36 Gt yr⁻¹ on average), with little seasonal variability relative to the long-term trend. There is a small seasonal cycle in ISSM dynamics driven by the SMB cycle (visible in the detrended timeseries shown in Fig. S3) which complements the mass changes from MAR (increased mass loss from MAR leads to decreased mass loss from ISSM, and vice versa), with an amplitude roughly an order of magnitude smaller than the SMB fluctuations. Together, ISSM and MAR v3.5.2 results produce a net loss of mass over 2003-2012, although the trend in simulated mass loss (-178.9 ± 4.49 Gt yr⁻¹) is smaller in magnitude than that of GRACE-LM (-239.4 ± 7.740 Gt yr⁻¹) by 60.5 ± 12.14 Gt yr⁻¹.

The roughly complementary nature of modeled SMB and DMB is evident on a sub ice-sheet wide scale, as indicated by the unfiltered MAR v3.5.2 and ISSM 2003-2012 mean SMB and DMB (Fig. 1) as well as the Gaussian filtered data (Figs. 7a and 7b). Areas with a large positive SMB from MAR v3.5.2 show large dynamic mass loss from ISSM (e.g. areas higher than 2000 m in elevation), while areas with negative SMB from MAR v3.5.2 show smaller losses from ISSM. Summing SMB and DMB from MAR v3.5.2 and ISSM produces the pattern of MB shown in Fig. 7c, which indicates that the majority of modeled mass loss for the 2003-2012 period occurs below 2000 m in elevation. This is similar to pattern of MB from GRACE-LM (Fig. 7d). A map of the difference between modeled and GRACE-LM MB (Fig. 7e) indicates that the majority of the difference in trends observed in Fig. 6 results from an underestimation of mass loss from the filtered model resultss below 2000 m in elevation, in particular along the west and southeast coasts. Mass loss from GRACE-LM is larger in magnitude along the GrIS margins (by up to ~ 2.5 Gt yr⁻¹ per mascon). In areas below 2000 m, overall mass loss is underestimated by 92 ± 10.3 Gt yr⁻¹ (with a trend of -149.4 ± 3.550 Gt yr⁻¹ as compared with -242.4 ± 6.8 Gt yr⁻¹ from GRACE). For areas above 2000 m, GRACE-LM suggests little change in mass (a mass gain of $+3.0 \pm 4.2$ Gt yr⁻¹), while the models suggest a loss of $-30-29.5 \pm 1.0$ Gt yr⁻¹. The differences between the models and GRACE-

LM are larger than the uncertainties in trends from GRACE-LM and from the model outputs, suggesting that model errors or unaccounted-for processes contribute to the difference.

The differences between simulated and GRACE-LM MB may be due to a modeled MAR v3.5.2 SMB that is too high below 2000 m in elevation, or alternately, to simulated velocities that are underestimated in ISSM and vice versa at higher elevations. We evaluate the ISSM spin-up by comparing the ISSM ice thickness at steady-state to the ice thickness obtained from the mass conservation dataset of Morlighem et al. (2015), derived from radar data for 1993-2014, interpolated onto the ISSM mesh. We also compare ISSM annual ice velocities with the radar-derived ice velocity data of Rignot and Mouginot (2012), derived from data spanning 2008-2009.

—A comparison of ice thicknesses from Morlighem et al. (2015) and velocities from Rignot and Mouginot (2012) with ISSM velocities and thicknesses for 1 January 2003 is shown in Fig. S4. Some differences may result from the model outputs and observations not being coincident in time, but Fig. S3 indicates that temporal variability in ISSM is small (<10%) relative to long-term changes. (This relatively small variability is to be expected given that the ISSM simulation used here only considers forcing from SMB and not other factors that may lead to larger fluctuations in ice motion.) In particular, ice velocities tend to be underestimated for glaciers along the northwest coast of the GrIS (Fig. S4b), possibly as a consequence of an upstream ice thickness that is also underestimated (Fig. S4a). This may contribute to underestimated mass loss along the northwest coast. In other areas, ice thickness is generally overestimated by ISSM, but some outlet glacier velocities are overestimated while others are underestimated, making it unclear how ISSM contributes to the observed discrepancies in these regions— the ice thickness is underestimated in central northwestern Greenland, but overestimated along the coast and in southern Greenland. In areas of underestimated thickness, ISSM velocities tend to be underestimated, resulting in a dynamic accumulation of mass that should be leaving the ice sheet.

It is difficult to determine if the observed differences are a result of errors in the MAR v3.5.2 SMB forcing (as the spinup relies primarily on the simulated SMB for forcing), simplifications to full-Stokes ice flow in ISSM, processes not considered in the ISSM simulation such as the role of hydrology in ice dynamics and ice-ocean interactions, or errors associated with the assumption that during the spin-up period, the ice sheet is in steady state. The assumption of 2D flow (the Shelfy-Stream Approximation SSA) in the current ISSM simulation probably contributes to errors in dynamic mass balance, particularly at higher elevations, but it is not clear whether this would lead to faster or slower ice flow. A comparison between MAR v3.5.2 SMB and in

situ measurements performed by Colgan et al. (2015) suggests that MAR v3.5.2 does not overestimate SMB below 2000 m, but this comparison is limited to one location in southwest Greenland: the Kangerlussuaq transect (van de Wal et al., 2005), and may not be representative of other areas. Another factor that may result in the discrepancy between model results and GRACE-LM is the 25 km resolution of the MAR outputs used in this study. ISSM is forced by a downscaled version of MAR v3.5.2. Using a higher resolution simulation or downscaled outputs could result in different SMB estimates (e.g. Franco et al., 2012). This could be particularly important along the borders of the GrIS, or for mountainous areas outside the ice sheet boundaries. In these areas, high spatial variability of topography can strongly influence SMB. To properly identify the source of the differences, further independent evaluations of MAR SMB and ISSM DMB are needed, for example, comparison between ISSM and remote-sensing derived discharge estimates (e.g. Rignot and Kanagaratnam, 2006), or comparison between MAR and additional in situ measurements in ablation areas.

3.2 Seasonal mass changes from MAR, ISSM and GRACE

The average seasonal cycle of filtered cumulative MAR v3.5.2 + ISSM for the 2003 through 2012 period agrees well with that of GRACE-LM, as shown in Fig. 8a and Table 2. The amount of mass loss during the period of net ablation is similar for MAR v3.5.2 + ISSM (333 Gt) and GRACE-LM (355 ± 32 Gt). The dates of simulated maximum and minimum mass fall within the range of uncertainty for these dates from GRACE-LM. It is possible, however, that differences in modeled and GRACE-LM trends alter the timing of the seasonal cycle, because changing the overall trend of a timeseries can alter the timing of local maxima and minima by altering local rates of change. Therefore, we also show the seasonal cycle for the de-trended timeseries in Fig. 8b and Table 2. For the de-trended seasonal cycle, the timing of the seasonal maximum occurs roughly 1 month before the maximum peak from the original seasonal cycle, and the timing of the seasonal minimum occurs roughly 1 week earlier (within the uncertainty associated with the ~10 day GRACE timesteps) for both MAR v3.5.2 + ISSM and GRACE-LM. ~~The~~In either case, the model timing for the filtered model data falls within the range of dates from GRACE-LM (with and without trends removed), and therefore we cannot confirm any difference between the modeled and GRACE-LM Greenland-wide seasonal cycles of mass change. The results are consistent with the comparison between the detrended MAR v3.5.2 and MAR v2.0 seasonal cycles and GRACE. ISSM makes a small

contribution to the simulated seasonal cycle; its seasonal cycle is the inverse of the MAR seasonal cycle with a lag of less than 1 month, indicating that ISSM responds to MAR SMB forcing by increasing discharge during periods of high SMB, and vice versa, with an amplitude roughly an order of magnitude smaller than that of MAR (Fig. S5). As noted earlier, this magnitude of simulated flow variability is the expected response to the SMB forcing applied to ISSM.

3.3 Spatial variability in the seasonal cycle from MAR, ISSM and GRACE

Maps of the timing of peaks in the seasonal cycle of de-trended cumulative mass change from GRACE-LM (Fig. 9) suggest that the timing of seasonal cycle peaks is spatially variable. Maps of the median GRACE-LM date for the maximum and minimum peaks (Figs. 9a and d) show that in some locations (e.g. northwest Greenland), GRACE-LM suggests that the peak in the seasonal cycle can occur as early as ~~November~~ 11 November (i.e. mass loss begins during the fall), where in other areas it occurs as late as ~~July~~ 11 July (for an area in north Greenland). The range of possible dates suggested by ~~95% of the GRACE-LM distribution~~ GRACE-LM, when taking into account GRACE-LM uncertainty, is fairly large, spanning ~~the full November 1 to July 1 period~~ up to 5 months in some locations in northern Greenland (Figs. 9b, c, e and f), but spatial differences in seasonal timing are preserved even with these large ranges. The GRACE-LM data suggest that the period of net mass loss begins in ~~late winter~~ fall and ends in early summer in the northwestern portion of the ice sheet, while in most other parts of the ice sheet, mass loss begins in early or late spring, and mass begins to increase again beginning in ~~mid to~~ late autumn. The period of summer mass loss over most of the ice sheet is consistent with what would be expected, given the cycle of climate forcing (warm conditions leading to increased melt), but the timing of the cycle in the northwest suggests that other processes may dominate seasonal variability in that region.

MAR v3.5.2 + ISSM suggest a more uniform pattern of timing in seasonal cycle peaks (Figs. 10a, b), consistent with the SMB forcing. The ~~models suggest~~ filtered model results suggest that mass loss begins in late spring and early summer (between March and June) without much spatial variability across the ice sheet, and mass gain commences in late summer and early fall (between September and November), with the period of mass loss ending ~1 month later for mascons below 2000 m in elevation relative to those above 2000 m in elevation. These results are consistent with what would be expected given warmer temperatures at lower

elevations and a longer period available for melting. (The differences are also likely to be larger without filtering.)

For many mascons in the Northwest, the modeled cycle maximum and minimum peaks can occur up to 3 months after and 2 months before the GRACE-LM peaks (Figs. 10c, d), with differences of ~1 month being quite common. Given the relatively large uncertainty in the timing of the GRACE-LM peaks, the model peaks often fall within the distribution of peaks from GRACE-LM. Along the northwest coast, however, the timing of the seasonal maximum occurs in May according to the models, roughly one or two months after the 95% confidence limit on the timing of maximum mass from GRACE-LM, and more than three months after the median peak from GRACE-LM. — The clustering of the GRACE-LM peaks, despite the large uncertainty in the GRACE timing, suggests that the observed variations in timing are not associated with random deviations between mascons, but reflect seasonal variations in mass detected by GRACE-LM, that are not captured by the models. Despite the large uncertainty in the GRACE timing, the timing of GRACE-LM peaks tends to be clustered in groups, suggesting that the spatial variations in GRACE-LM timing are not random, but actually reflect seasonal variations in mass not captured by the models.—The timing of seasonal minimum falls within 95% of the distribution from GRACE-LM, with the exception of ~~six mascons at high elevations along the southeast coast.~~ four mascons in the northwest GrIS region.

3.4 The average seasonal cycle within ice sheet sub-regions

In order to further examine discrepancies at regional scales, we created ~~eight-nine~~ sub-regions of the GrIS based on the median timing of the maximum and minimum peaks of the average de-trended annual cycle from GRACE-LM (Figs. 9a and d). Mascons were grouped together if the timing of their maximum and minimum peaks were within ~~340~~ days of each other. (The threshold was chosen to create a balance between different types cyclical patterns and the number of total regions.)—The ~~eight-nine~~ sub-regions are shown in Fig. 11a, along with the average seasonal cycle from four of these sub-regions (Figs. 11b-e). The average cycles for other regions are provided in Figs. S6a-~~ed~~. The average GRACE-LM seasonal cycle for Region ~~24~~ significantly differs in its timing from the MAR v3.5.2 + ISSM cycle. GRACE-LM results suggest that the period of net mass loss begins no later than mid-February, while the models suggest that it begins in ~~mid-April~~ late April as a result of the SMB signal. For Region ~~76~~ (Fig. 11e), the ~~maximum modeled mass~~ maximum in the cycle of cumulative mass

~~change~~ occurs in ~~early-mid~~ May (although the ice sheet does not appear to start losing a substantial amount of mass until ~~July~~late June), while the GRACE-LM peak occurs ~~in-early~~ ~~November~~in mid February. The entire modeled cycle appears to be offset by three months relative to GRACE-LM in this region, although seasonal mass changes are relatively small (on the order of 5 Gt). For Regions ~~54~~ and ~~65~~ (Figs. 11c and d), the model maximum and minimum peaks fall within the distribution for GRACE-LM peaks. For Regions ~~12~~, ~~37~~ and 8 (Figs. S6a, ~~be~~, and d) the cycles are similar to those of Regions ~~24~~ and ~~76~~. For Region ~~43~~ (Fig. S6~~cb~~), the cycle is similar to the cycle of Region ~~64~~, except for a sharp peak in mass in early July, which leads the GRACE-LM peak to occur after the peak from the models. ~~For Region 9 (Fig. S6e) the GRACE-LM maximum peak is similar to that of other regions in northwest Greenland, preceding the model maximum peak, but the minimum GRACE-LM peak overlaps with a September minimum peak from the models.~~

Dividing the GrIS into high and low elevation areas (above and below 2000 m in elevation) also produces differences in the seasonal cycle (Fig. 12). For areas below 2000 m in elevation (Fig. 12a), there is a good agreement between the GRACE-LM and simulated seasonal cycles; the timing of MAR v3.5 + ISSM maximum and minimum peaks fall within the distribution of peaks for GRACE-LM as the signal is dominated by the summer surface mass loss. For areas higher than 2000 m in elevation (Fig. 12b), the period of simulated net mass loss is shortened relative to that of GRACE-LM. —The good agreement between cycles at low elevations suggests that the timing of ablation and accumulation at low elevations on an ice sheet wide scale is well captured by MAR v3.5.2 + ISSM.

As for Greenland-wide fluctuations in mass, most of the simulated seasonal variability within sub-regions of the ice sheet is dominated by MAR, as expected given that the only forcing applied to ISSM is the SMB from MAR. ISSM exhibits a seasonal cycle that is a lagged inverse of the MAR cycle with less than 10% of the amplitude of MAR v3.5.2 in all sub-regions of the ice sheet (Figs. S7, S8, and S9), and the seasonal response is consistent across all areas of the ice sheet. The timing of the seasonal cycle for GRACE, MAR v3.5.2, ISSM, and MAR v3.5.2+ISSM for all sub-regions is provided in Table S1.

The differences in the GRACE-LM and modeled seasonal cycles within individual regions ~~and at high elevations~~ seem unlikely to be caused by errors in the simulated timing of surface ablation, as they occur either during times of the year when melting does not occur at the surface (i.e. the ‘early’ start to the period of net mass loss in the ~~northeast-northwest~~ from

November through February; Figs. 9a, b, c). ~~or in areas where the net ablation due to melting is small (i.e. above 2000 m in elevation).~~ The results therefore suggest that the observed changes could be associated with errors in seasonal accumulation from MAR v3.5.2, or processes not currently incorporated into ISSM, which induce seasonal fluctuations in ice discharge or liquid water. These processes are difficult to validate, and therefore it is difficult to determine which processes are most responsible for the observed differences. As discussed in the following section, significant seasonal variations in glacier velocities have been observed and could contribute to the observed discrepancies. Accumulation or ice flow errors could also affect differences at higher elevations, where the net ablation due to melting is small (i.e. above 2000 m in elevation). Such discrepancies could also be influenced by differences below 2000 m due to leakage between constraint regions, but the amount of leakage in terms of amplitude is small and is comparable to the GRACE-LM uncertainty (Luthcke et al., 2013). Additionally, it is possible that although the GRACE-LM solution includes error estimates associated with the forward models used in GRACE processing, ~~there is also a possibility that other non-ice-sheet-related processes may contribute to the differences-unaccounted for errors or processes, such as errors in model simulations used to correct for variability in atmospheric or ocean circulation (for which observations for validation are limited) may contribute to the differences.~~ However, we cannot envision any obvious reason for the discrepancy other than the potential errors in ISSM or MAR v3.5.2 that have been noted.

4 Discussion and Conclusions**Concluding remarks**

The above results show several areas of agreement as well as areas of disagreement between modeled and GRACE-derived Greenland mass balance. We have shown that in order to compare spatial and temporal variations in GrIS mass from RCM, ISM results and the GRACE-LM solution, it is necessary to spatially and temporally filter the model outputs. We have developed a Gaussian approximation to the GRACE-LM resolution operator, which accurately captures the effect of the GRACE-LM solution on spatial variations in mean MB. We also find that applying temporal filtering reduces differences between the modeled and GRACE-LM seasonal cycles. We have therefore ~~implemented a temporal Gaussian filter with the goal of reproducing this effect~~ also applied a temporal Gaussian filter to the model outputs to reproduce the attenuation inherent to GRACE-LM processing. The Gaussian temporal

1 filtering does not completely capture the seasonal cycle of mass changes obtained using the
2 GRACE-LM resolution operator in that it extends the period of mass loss simulated by the
3 models further than the period obtained from GRACE-LM filtering. As the filter extends the
4 length of the modeled period of mass loss, and tends to bring the timing of modeled seasonal
5 cycle peaks closer to those from GRACE-LM (which exhibits a longer period of mass loss
6 relative to the unfiltered model results), our approach is conservative: in cases where the
7 cycles disagree, there is likely a difference between the GRACE-LM and modeled seasonal
8 cycles.

9 ~~As the filter brings the timing of the Greenland-wide cycle of mass changes closer to that of~~
10 ~~GRACE-LM, in cases where it disagrees with the Greenland-wide cycle, differences in the~~
11 ~~timing of the modeled and GRACE-LM cycle are likely.~~

12 A comparison between Gaussian-filtered MAR v3.5.2 + ISSM and GRACE-LM Greenland
13 mass trends for 2003-2012 indicates that the models tend to underestimate the magnitude of
14 this mass loss, as a result of underestimated mass loss below 2000 m in elevation. This
15 difference is either due to an overestimation of SMB from MAR v3.5.2 in low elevation areas,
16 or to intrinsic errors in ice flow from ISSM. MAR v3.5.2 SMB for low elevation areas is
17 higher than that of MAR v2.0, in part due to a relatively high bare ice albedo (as described by
18 Alexander et al., 2014; a higher albedo persists despite modifications made to MAR v3.5.2
19 albedo), and in part due to a shift in precipitation from high to low elevation areas. A
20 comparison at eight in situ stations at the Kangerlussuaq transect on the southwest GrIS
21 suggests that MAR v3.5.2 SMB is closer to in situ measurements (Colgan et al., 2015), but
22 such measurements are limited to this transect with the exception of a comparable number of
23 ablation stake measurements from the Programme for Monitoring of the Greenland Ice Sheet
24 (PROMICE; www.promice.org). ~~few SMB measurements are available within the GrIS~~
25 ~~ablation area.~~—The only means of determining the relative contribution of ISSM and MAR
26 v3.5.2 to underestimated mass loss would be to conduct an independent evaluation of each
27 model against DMB (e.g. using the methods of Rignot and Kanagaratnam, 2006) and SMB
28 estimates over large portions of the GrIS. ~~These analyses are beyond the scope of this~~
29 ~~study beyond the scope of this study, and the evaluation of SMB is limited by sparsely~~
30 ~~available data, although radar measurements of snow accumulation may help to fill this gap.~~
31 A preliminary comparison by Koenig et al. (2015) suggests that there is a good agreement
32 between MAR v3.5.2 and radar-derived accumulation estimates over the interior of the GrIS

1 during the years 2009-2012, but that MAR tends to overestimate accumulation along the
2 southeastern coast.

3 We examined the mean seasonal cycles of de-trended cumulative mass change from GRACE-
4 LM and MAR v3.5.2 + ISSM as a means of examining the ability of the models to capture
5 mass changes at a relatively high spatial and temporal resolution. We have shown that on a
6 Greenland-wide scale, the timing of modeled and GRACE seasonal cycles agree, within the
7 limits of GRACE uncertainty, but on sub-ice-sheet-wide scales, there are significant
8 differences in the timing of annual cycle ~~peakspeak~~. On the scale of individual mascons, there
9 is considerable variability in the timing of the seasonal cycle ~~as represented by from~~ GRACE-
10 LM, while model ~~results-outputs~~ suggest a more uniform timing across Greenland driven
11 mainly by summer surface mass loss and mass gain simulated by MAR. While some of this
12 variability is likely due to GRACE errors, other variations likely reflect real differences in the
13 seasonal variability within different regions, particularly as the differences are not random,
14 but spatially clustered. In particular, in northwestern Greenland, the simulated period of mass
15 loss is shorter than that of GRACE-LM, and the timing of the simulated maximum in the
16 seasonal cycle occurs up to three months after the GRACE-LM peak in some areas.

17 Spatial and seasonal differences in the seasonal cycle may result from various factors
18 including (1) underestimation or overestimation of accumulation and ablation by MAR
19 v3.5.2, (2) cycles of ice sheet motion associated with processes not incorporated into ISSM,
20 (3) cycles of water storage and release, and (4) errors in the GRACE-LM solution. We have
21 attempted to account for the last factor by considering the impact of errors of the GRACE-LM
22 solution estimated by Luthcke et al. (2013) on the timing of the seasonal cycle, and by
23 filtering our model results to match GRACE-LM. However, as GRACE does not provide
24 direct observations of mass changes, and different methods of processing can produce
25 somewhat different mass change solutions (Shepherd et al., 2012), it is possible that some of
26 the observed discrepancies may be due to errors not considered in this solution. With regard
27 to MAR v3.5.2 accumulation, the Colgan et al. (2015) study suggests that MAR v3.5.2
28 effectively captures spatial variations in SMB, but few observations of SMB are available in
29 areas of net ablation. The seasonal cycle of MAR v3.5.2 has not been evaluated against
30 observations, as few sub-annual estimates of accumulation are available. With regard to GrIS
31 discharge, an analysis of ISSM annual discharge has not been conducted, although
32 comparison with satellite-derived ice velocities suggests that ISSM velocities may be

underestimated in some areas at the ice sheet margins. Data on seasonal velocities are not available for the entire GrIS, but various studies have indicated seasonal variations in the flow of GrIS glaciers occur, particularly in association with meltwater that reaches the ice sheet bed (e.g. Joughin et al., 2008), as well as interactions between ocean circulation and ice at calving fronts (Howat et al., 2010). Using GPS measurements for west coast GrIS glaciers, Ahlstrøm et al. (2013) showed that the glaciers examined underwent seasonal cycles in velocity, with several glaciers showing a decline in velocity in late summer associated with increased efficiency of subglacial drainage systems. Moon et al. (2014) present the most comprehensive evaluation of seasonal velocity cycles to date, identifying three types of seasonal cycles in velocity near the terminus of marine-terminating glaciers, one in which meltwater production produces acceleration during summer months (“type 2”), another in which deceleration occurs late in the melt season, followed by acceleration peaking in the early melt season (“type 3”), and a third in which fluctuations are more likely associated with ice-ocean interactions (“type 1”). Different glaciers exhibit different patterns of flow variability, and ~~may transition a single glacier may exhibit different patterns of flow in different years between different patterns in different years.~~ Seasonal variations in flow generally represent ~10-20% of mean annual velocities. The type 1 and especially type 3 seasonal patterns could potentially lead to the patterns of mass change from GRACE-LM in north~~west~~~~east~~ Greenland, but it is unclear how variations in flow of different glaciers contribute to seasonal fluctuations in ice sheet discharge, and a study examining this would be useful for evaluating ISMs such as ISSM, which do not currently take into account the influence of these processes.

The general agreement between modeled and GRACE-LM MB below 2000 m in elevation, where ice sheet hydrology might be expected to play a role, suggests that factors such as water storage and release as indicated by Rennermalm et al. (2013), and observed on glaciers in locations outside of Greenland (Jansson et al., 2003) do not play a large role in the timing of seasonal variations in mass on the ice-sheet-wide scale. It is possible that these processes influence the amplitude of mass variations, or lead to changes in mass on shorter timescales that we cannot observe given the uncertainties in GRACE-LM results and filtering, and that they play a role in longer-term variations in mass. Long-term water storage could contribute to underestimated trends in mass loss below 2000 m in elevation, which could also result from underestimated SMB from MAR v3.5.2, or an underestimation of D from ISSM.

Further studies are also needed to understand the impact of temporal variations in mass on the observations presented here, i.e. whether they are associated with processes that reoccur from year-to-year, or whether isolated events influence the timing of the seasonal cycle. In addition, future studies are needed to validate seasonal variations of RCM accumulation and simulated SMB in ablation areas. The spatial and temporal resolution of this analysis was limited by the fundamental spatial and temporal resolutions of GRACE to seasonal-scale variability and spatial scales of ~600 km. It is possible that if seasonal variations in GrIS mass are examined at higher spatial and temporal resolutions, with reduced errors, further discrepancies between modeled and measured cycles will be observed. As the ice sheet changes in the future, such processes could potentially become more important to GrIS-wide changes in mass, and therefore they need to be better understood and their impact quantified.

Author contribution

P. M. A. and M. T. devised the study. P. M. A. carried out the analysis. N-J. S. and E. L. performed simulations with and developed the ISSM model. S. L. produced the GRACE solution. X. F. performed simulations and development of the MAR model. P. M. A. prepared the manuscript. All co-authors revised and contributed to the editing of the manuscript.

Acknowledgements

P. Alexander and M. Tedesco were supported by NSF Grant PLR # 0909388. Work of N-J. Schlegel and E. Larour was performed at the California Institute of Technology's Jet Propulsion Laboratory under a contract with the National Aeronautics and Space Administration's Cryosphere Program. The authors would like to thank Rajashree Datta, Dr. Erik Noble, and Erik Orantes of the Cryospheric Processes Laboratory and two anonymous reviewers for their valuable comments and suggestions.

References

- Ahlstrøm, A. P., Andersen, S. B., Andersen, M. L., Machguth, H., Nick, F. M., Joughin, I., Reijmer, C. H., van de Wal, R. S. W., Merryman Boncori, J. P., Box, J. E., Citterio, M., van As, D., Fausto, R. S. and Hubbard, A.: Seasonal velocities of eight major marine-terminating outlet glaciers of the Greenland ice sheet from continuous in situ GPS instruments, *Earth Syst. Sci. Data*, 5(2), 277–287, doi:10.5194/essd-5-277-2013, 2013.
- Alexander, P. M., Tedesco, M., Fettweis, X., van de Wal, R. S. W., Smeets, C. J. P. P. and van den Broeke, M. R.: Assessing spatio-temporal variability and trends in modelled and measured Greenland Ice Sheet albedo (2000–2013), *The Cryosphere*, 8(6), 2293–2312, doi:10.5194/tc-8-2293-2014, 2014.
- Bartholomew, I., Nienow, P., Mair, D., Hubbard, A., King, M. A. and Sole, A.: Seasonal evolution of subglacial drainage and acceleration in a Greenland outlet glacier, *Nat. Geosci.*, 3(6), 408–411, doi:10.1038/ngeo863, 2010.
- Box, J. E.: Greenland Ice Sheet Mass Balance Reconstruction. Part II: Surface Mass Balance (1840–2010), *J. Clim.*, 26(18), 6974–6989, doi:10.1175/JCLI-D-12-00518.1, 2013.
- Box, J. E., Cressie, N., Bromwich, D. H., Jung, J.-H., van den Broeke, M., van Angelen, J. H., Forster, R. R., Miège, C., Mosley-Thompson, E., Vinther, B. and McConnell, J. R.: Greenland Ice Sheet Mass Balance Reconstruction. Part I: Net Snow Accumulation (1600–2009), *J. Clim.*, 26(11), 3919–3934, doi:10.1175/JCLI-D-12-00373.1, 2013.
- Brun, E., David, P., Sudul, M. and Brunot, G.: A numerical model to simulate snow-cover stratigraphy for operational avalanche forecasting, *J. Glaciol.*, 38(128), 13–22, 1992.
- Chu, V. W.: Greenland ice sheet hydrology: A review, *Prog. Phys. Geogr.*, 38(1), 19–54, doi:10.1177/0309133313507075, 2014.
- Colgan, W., Box, J. E., Andersen, M. L., Fettweis, X., Csathó, B., Fausto, R. S., van As, D., and Wahr, J.: Greenland high-elevation mass balance: inference and implication of reference period (1961–90) imbalance, *Ann. Glaciol.*, 56(70), 105–117, doi:10.3189/2015AoG70A967, 2015.
- Cuffey, K. M. and Paterson, S. B.: Chapter 4: Mass Balance Processes: 1. overview and regimes, in: *The Physics of Glaciers*, Academic Press, Oxford, UK, 91–136, 2011.
- Das, S. B., Joughin, I., Behn, M. D., Howat, I. M., King, M. A., Lizarralde, D. and Bhatia, M. P.: Fracture Propagation to the Base of the Greenland Ice Sheet During Supraglacial Lake Drainage, *Science*, 320(5877), 778–781, doi:10.1126/science.1153360, 2008.
- Dee, D. P., Uppala, S. M., Simmons, A. J., Berrisford, P., Poli, P., Kobayashi, S., Andrae, U., Balmaseda, M. A., Balsamo, G., Bauer, P., Bechtold, P., Beljaars, A. C. M., van de Berg, L., Bidlot, J., Bormann, N., Delsol, C., Dragani, R., Fuentes, M., Geer, A. J., Haimberger, L., Healy, S. B., Hersbach, H., Hólm, E. V., Isaksen, L., Kållberg, P., Köhler, M., Matricardi, M., McNally, A. P., Monge-Sanz, B. M., Morcrette, J.-J., Park, B.-K., Peubey, C., de Rosnay, P., Tavolato, C., Thépaut, J.-N. and Vitart, F.: The ERA-Interim reanalysis: configuration and performance of the data assimilation system, *Q. J. R. Meteorol. Soc.*, 137(656), 553–597, doi:10.1002/qj.828, 2011.

1 Ettema, J., van den Broeke, M. R., van Meijgaard, E., van de Berg, W. J., Bamber, J. L., Box,
2 J. E. and Bales, R. C.: Higher surface mass balance of the Greenland ice sheet revealed by
3 high-resolution climate modeling, *Geophys. Res. Lett.*, 36, L12501,
4 doi:10.1029/2009GL038110, 2009.

5 Fettweis, X.: Reconstruction of the 1979-2006 Greenland ice sheet surface mass balance
6 using the regional climate model MAR, *The Cryosphere*, 1, 21–40, 2007.

7 Fettweis, X., Hanna, E., Lang, C., Belleflamme, A., Erpicum, M. and Gallée, H.: Brief
8 communication: “Important role of the mid-tropospheric atmospheric circulation in the recent
9 surface melt increase over the Greenland ice sheet,” *The Cryosphere*, 7(1), 241–248,
10 doi:10.5194/tc-7-241-2013, 2013a.

11 Fettweis, X., Franco, B., Tedesco, M., van Angelen, J. H., Lenaerts, J. T. M., van den Broeke,
12 M. R. and Gallée, H.: Estimating the Greenland ice sheet surface mass balance contribution to
13 future sea level rise using the regional atmospheric climate model MAR, *The Cryosphere*,
14 7(2), 469–489, doi:10.5194/tc-7-469-2013, 2013b.

15 Forster, R. R., Box, J. E., van den Broeke, M. R., Miège, C., Burgess, E. W., van Angelen, J.
16 H., Lenaerts, J. T. M., Koenig, L. S., Paden, J., Lewis, C., Gogineni, S. P., Leuschen, C. and
17 McConnell, J. R.: Extensive liquid meltwater storage in firn within the Greenland ice sheet,
18 *Nat. Geosci.*, 7(2), 95–98, doi:10.1038/ngeo2043, 2013.

19 Franco, B., Fettweis, X., Lang, C. and Erpicum, M.: Impact of spatial resolution on the
20 modelling of the Greenland ice sheet surface mass balance between 1990–2010, using the
21 regional climate model MAR, *The Cryosphere*, 6(3), 695–711, doi:10.5194/tc-6-695-2012,
22 2012.

23 Franco, B., Fettweis, X. and Erpicum, M.: Future projections of the Greenland ice sheet
24 energy balance driving the surface melt, *The Cryosphere*, 7(1), 1–18, doi:10.5194/tc-7-1-
25 2013, 2013.

26 Gallée, H.: Air-sea interactions over Terra Nova Bay during winter: simulation with a coupled
27 atmosphere-polynya model, *J. Geophys. Res.*, 102, 13835–13849, 1997.

28 Gallée, H. and Schayes, G.: Development of a three-dimensional meso- γ primitive equation
29 model: katabatic winds simulation in the area of Terra Nova Bay, Antarctica, *Mon. Weather*
30 *Rev.*, 122, 671–685, 1994.

31 Hoffman, M. J., Catania, G. A., Neumann, T. A., Andrews, L. C. and Rumrill, J. A.: Links
32 between acceleration, melting, and supraglacial lake drainage of the western Greenland Ice
33 Sheet, *J. Geophys. Res.*, 116, F04035, doi:10.1029/2010JF001934, 2011.

34 Howat, I. M., Box, J. E., Ahn, Y., Herrington, A. and McFadden, E. M.: Seasonal variability
35 in the dynamics of marine-terminating outlet glaciers in Greenland, *J. Glaciol.*, 56(198), 601–
36 613, 2010.

37 Huybrechts, P., Goelzer, H., Janssens, I., Driesschaert, E., Fichefet, T., Goosse, H. and
38 Loutre, M.-F.: Response of the Greenland and Antarctic Ice Sheets to Multi-Millennial
39 Greenhouse Warming in the Earth System Model of Intermediate Complexity LOVECLIM,
40 *Surv. Geophys.*, 32(4-5), 397–416, doi:10.1007/s10712-011-9131-5, 2011.

- 1 Jansson, P., Hock, R. and Schneider, T.: The concept of glacier storage: a review, *J. Hydrol.*,
2 282(1-4), 116–129, doi:10.1016/S0022-1694(03)00258-0, 2003.
- 3 Joughin, I., Das, S. B., King, M. A., Smith, B. E., Howat, I. M. and Moon, T.: Seasonal
4 Speedup Along the Western Flank of the Greenland Ice Sheet, *Science*, 320(5877), 781–783,
5 doi:10.1126/science.1153288, 2008.
- 6 Joughin, I., Smith, B. E., Shean, D. E. and Floricioiu, D.: Brief Communication: Further
7 summer speedup of Jakobshavn Isbræ, *The Cryosphere*, 8(1), 209–214, doi:10.5194/tc-8-209-
8 2014, 2014.
- 9 Koenig, L. S., Miège, C., Forster, R. R. and Brucker, L.: Initial in situ measurements of
10 perennial meltwater storage in the Greenland firn aquifer, *Geophys. Res. Lett.*, 41(1), 81–85,
11 doi:10.1002/2013GL058083, 2014.
- 12 Koenig, L. S., Ivanoff, A., Alexander, P. M., MacGregor, J. A., Fettweis, X., Panzer, B.,
13 Paden, J. D., Forster, R. R., Das, I., McConnell, J., Tedesco, M., Leuschen, C., and Gogineni,
14 P.: Annual Greenland accumulation rates (2009-2012) from airborne Snow Radar, *The*
15 *Cryosphere Discuss.*, 9, 6697-6731, doi: 10.5194/tcd-9-6697-2015, 2015.
- 16
- 17 Larour, E., Seroussi, H., Morlighem, M. and Rignot, E.: Continental scale, high order, high
18 spatial resolution, ice sheet modeling using the Ice Sheet System Model (ISSM), *J. Geophys.*
19 *Res.*, 117, F01022, doi:10.1029/2011JF002140, 2012.
- 20 Lefebre, F., Gallée, H., van Ypersele, J.-P. and Greuell, W.: Modeling of snow and ice melt at
21 ETH Camp (West Greenland): a study of surface albedo, *J. Geophys. Res.*, 108, 4321,
22 doi:10.1029/2001JD001160, 2003.
- 23 Luthcke, S. B., Zwally, H. J., Abdalati, W., Rowlands, D. D., Ray, R. D., Nerem, R. S.,
24 Lemoine, F. G., McCarthy, J. J. and Chinn, D. S.: Recent Greenland Ice Mass Loss by
25 Drainage System from Satellite Gravity Observations, *Science*, 314(5803), 1286–1289,
26 doi:10.1126/science.1130776, 2006.
- 27 Luthcke, S. B., Sabaka, T. J., Loomis, B. D., Arendt, A. A., McCarthy, J. J. and Camp, J.:
28 Antarctica, Greenland and Gulf of Alaska land-ice evolution from an iterated GRACE global
29 mascon solution, *J. Glaciol.*, 59(216), 613–631, doi:10.3189/2013JoG12J147, 2013.
- 30 MacAyeal, D. R.: Large-scale ice flow over a viscous basal sediment: theory and application
31 to ice stream B, Antarctica, *J. Geophys. Res.*, 94(B4), 4071–4087, 1989.
- 32 Moon, T., Joughin, I., Smith, B., van den Broeke, M. R., van de Berg, W. J., Noël, B. and
33 Usher, M.: Distinct patterns of seasonal Greenland glacier velocity: Seasonal velocity,
34 *Geophys. Res. Lett.*, 41(20), 7209–7216, doi:10.1002/2014GL061836, 2014.
- 35 Morlighem, M., Rignot, E., Seroussi, H., Larour, E., Ben Dhia, H. and Aubry, D.: Spatial
36 patterns of basal drag inferred using control methods from a full-Stokes and simpler models
37 for Pine Island Glacier, West Antarctica, *Geophys. Res. Lett.*, 37(14), L14502,
38 doi:10.1029/2010GL043853, 2010.

- 1 Morlighem, M., Rignot, E., Mouginot, J., Seroussi, H., and Larour, E.: High-resolution ice-
2 thickness mapping in South Greenland. *Ann. Glaciol.*, 55, 64–70,
3 doi:10.389/2014AoG67A088, 2014.
- 4 Morlighem, M., Rignot, E., Bouginot, J., Seroussi, H., and Larour, E.: IceBridge BedMachine
5 Greenland, Version 2. Boulder Colorado USA. NASA National Snow and Ice Data Center
6 Distributed Active Archive Center, doi:10.5067/AD7B0HQNSJ29, 2015.
- 7 Nghiem, S. V., Hall, D. K., Mote, T. L., Tedesco, M., Albert, M. R., Keegan, K., Shuman, C.
8 A., DiGirolamo, N. E. and Neumann, G.: The extreme melt across the Greenland ice sheet in
9 2012, *Geophys. Res. Lett.*, 39(20), L20502, doi:10.1029/2012GL053611, 2012.
- 10 Quiquet, A., Punge, H. J., Ritz, C., Fettweis, X., Gallée, H., Kageyama, M., Krinner, G., Salas
11 y Mélia, D. and Sjolte, J.: Sensitivity of a Greenland ice sheet model to atmospheric forcing
12 fields, *The Cryosphere*, 6(5), 999–1018, doi:10.5194/tc-6-999-2012, 2012.
- 13 Rennermalm, A. K., Smith, L. C., Chu, V. W., Box, J. E., Forster, R. R., Van den Broeke, M.
14 R., Van As, D. and Moustafa, S. E.: Evidence of meltwater retention within the Greenland ice
15 sheet, *The Cryosphere*, 7(5), 1433–1445, doi:10.5194/tc-7-1433-2013, 2013.
- 16 [Rignot, E., and Kanagaratnam, P.: Changes in the velocity structure of the Greenland Ice](#)
17 [Sheet, *Science*, 311, 986-990, doi: 10.1126/science.1121381, 2006.](#)
- 18 Rignot, E., and Mouginot, J.: Ice flow in Greenland for the International Polar Year 2008-
19 2009, *Geophys. Res. Lett.*, 39, L11501, doi: 10.1029/2012GL051634, 2012.
- 20 Rignot, E., Velicogna, I., van den Broeke, M. R., Monaghan, A. and Lenaerts, J. T. M.:
21 Acceleration of the contribution of the Greenland and Antarctic ice sheets to sea level rise,
22 *Geophys. Res. Lett.*, 38(5), L05503, doi:10.1029/2011GL046583, 2011.
- 23 Rignot, E., Fenty, I., Menemenlis, D. and Xu, Y.: Spreading of warm ocean waters around
24 Greenland as a possible cause for glacier acceleration, *Ann. Glaciol.*, 53(60), 257–266,
25 doi:10.3189/2012AoG60A136, 2012.
- 26 Robinson, A., Calov, R. and Ganopolski, A.: Greenland ice sheet model parameters
27 constrained using simulations of the Eemian Interglacial, *Clim. Past*, 7(2), 381–396,
28 doi:10.5194/cp-7-381-2011, 2011.
- 29 Sabaka, T. J., Rowlands, D. D., Luthcke, S. B. and Boy, J.-P.: Improving global mass flux
30 solutions from Gravity Recovery and Climate Experiment (GRACE) through forward
31 modeling and continuous time correlation, *J. Geophys. Res.*, 115, B11403,
32 doi:10.1029/2010JB007533, 2010.
- 33 Schlegel, N. J., Larour, E., Seroussi, H., Morlighem, M. and Box, J. E.: Decadal-scale
34 sensitivity of Northeast Greenland ice flow to errors in surface mass balance using ISSM, *J.*
35 *Geophys. Res. Earth Surf.*, 118(2), 667–680, 2013.
- 36 Schlegel, N.-J., Larour, E., Seroussi, H., Morlighem, M., and Box, J. E.: Ice discharge
37 uncertainties in Northeast Greenland from boundary conditions and climate forcing of an ice
38 flow model, *J. Geophys. Res. - Earth Surface*, 120, 29–54, doi:10.1002/2014JF003359, 2015.
- 39 Shepherd, A., Ivins, E. R., A, G., Barletta, V. R., Bentley, M. J., Bettadpur, S., Briggs, K. H.,
40 Bromwich, D. H., Forsberg, R., Galin, N., Horwath, M., Jacobs, S., Joughin, I., King, M. A.,

- 1 Lenaerts, J. T. M., Li, J., Ligtenberg, S. R. M., Luckman, A., Luthcke, S. B., McMillan, M.,
2 Meister, R., Milne, G., Mouginot, J., Muir, A., Nicolas, J. P., Paden, J., Payne, A. J.,
3 Pritchard, H., Rignot, E., Rott, H., Sorensen, L. S., Scambos, T. A., Scheuchl, B., Schrama, E.
4 J. O., Smith, B., Sundal, A. V., van Angelen, J. H., van de Berg, W. J., van den Broeke, M.
5 R., Vaughan, D. G., Velicogna, I., Wahr, J., Whitehouse, P. L., Wingham, D. J., Yi, D.,
6 Young, D. and Zwally, H. J.: A Reconciled Estimate of Ice-Sheet Mass Balance, *Science*,
7 338(6111), 1183–1189, doi:10.1126/science.1228102, 2012.
- 8 Smith, L. C., Chu, V. W., Yang, K., Gleason, C. J., Pitcher, L. H., Rennermalm, A. K.,
9 Legleiter, C. J., Behar, A. E., Overstreet, B. T., Moustafa, S. E., Tedesco, M., Forster, R. R.,
10 LeWinter, A. L., Finnegan, D. C., Sheng, Y. and Balog, J.: Efficient meltwater drainage
11 through supraglacial streams and rivers on the southwest Greenland ice sheet, *Proc. Natl.*
12 *Acad. Sci.*, 112(4), 1001–1006, doi:10.1073/pnas.1413024112, 2015.
- 13 Sundal, A. V., Shepherd, A., Nienow, P., Hanna, E., Palmer, S. and Huybrechts, P.: Melt-
14 induced speed-up of Greenland ice sheet offset by efficient subglacial drainage, *Nature*,
15 469(7331), 521–524, doi:10.1038/nature09740, 2011.
- 16 Tapley, B. D., Bettadpur, S., Ries, J. C., Thompson, P. F. and Watkins, M. M.: GRACE
17 measurements of mass variability in the Earth system, *Science*, 305(5683), 503–505, 2004.
- 18 Tedesco, M., Serreze, M. and Fettweis, X.: Diagnosing the extreme surface melt event over
19 southwestern Greenland in 2007, *The Cryosphere*, 2, 159–166, 2008.
- 20 Tedesco, M., Fettweis, X., van den Broeke, M. R., van de Wal, R. S. W., Smeets, C. J. P. P.,
21 van de Berg, W. J., Serreze, M. C. and Box, J. E.: The role of albedo and accumulation in the
22 2010 melting record in Greenland, *Environ. Res. Lett.*, 6(1), 014005, doi:10.1088/1748-
23 9326/6/1/014005, 2011.
- 24 Tedesco, M., Fettweis, X., Mote, T., Wahr, J., Alexander, P., Box, J. E. and Wouters, B.:
25 Evidence and analysis of 2012 Greenland records from spaceborne observations, a regional
26 climate model and reanalysis data, *The Cryosphere*, 7(2), 615–630, doi:10.5194/tc-7-615-
27 2013, 2013a.
- 28 Tedesco, M., Willis, I. C., Hoffman, M. J., Banwell, A. F., Alexander, P. and Arnold, N. S.:
29 Ice dynamic response to two modes of surface lake drainage on the Greenland ice sheet,
30 *Environ. Res. Lett.*, 8(3), 034007, doi:10.1088/1748-9326/8/3/034007, 2013b.
- 31 van den Broeke, M., Bamber, J., Ettema, J., Rignot, E., Schrama, E., van de Berg, W. J., van
32 Meijgaard, E., Velicogna, I. and Wouters, B.: Partitioning Recent Greenland Mass Loss,
33 *Science*, 326(5955), 984–986, doi:10.1126/science.1178176, 2009.
- 34 | van de Wal, R. S. W., Greuell, W., van den Broeke, M., Reijmer, C. H., and Oerlemans, J.:
35 Surface mass-balance observations and automatic weather station data along a transect near
36 Kangerlussuaq West Greenland, *Ann. Glaciol.*, 52, 311–316, doi:
37 10.3189/172756405781812529, 2005.
- 38 Velicogna, I. and Wahr, J.: Acceleration of Greenland ice mass loss in spring 2004, *Nature*,
39 443(7109), 329–331, doi:10.1038/nature05168, 2006.

1 Vernon, C. L., Bamber, J. L., Box, J. E., van den Broeke, M. R., Fettweis, X., Hanna, E. and
2 Huybrechts, P.: Surface mass balance model intercomparison for the Greenland ice sheet, *The*
3 *Cryosphere*, 7(2), 599–614, doi:10.5194/tc-7-599-2013, 2013.

4 Zwally, H. J., Abdalati, W., Herring, T., Larson, K., Saba, J. and Steffen, K.: Surface melt-
5 induced acceleration of Greenland Ice-Sheet Flow, *Science*, 297, 218–222, 2002.

6

7

Table 1. Timing of maximum and minimum peaks in the seasonal cycle of GrIS-wide detrended cumulative mass change for GRACE-LM and MAR v2.0 for the January 2003 – December -2010 period. For GRACE-LM, the median value and bounds for the 95% confidence interval of the distribution after accounting for uncertainty in GRACE-LM are listed. The uncertainty bounds have been extended by 10 days to account for potential errors associated with temporal resolution.

	GRACE	MAR v2.0 Unfiltered	MAR v3.5.2 Unfiltered	MAR v2.0 GRACE- Filtered	MAR v2.0 Gaussian- (Spatial)	MAR v2.0 Gaussian- (Space, Time)	MAR v3.5.2 Gaussian- (Space, Time)
Maximum (2.5% Bound)	29 Mar 26 Mar						
Maximum	30 27 Apr	19 May	22 May	10 9 May	19 May	29 Apr	1 May
Maximum (97.5% Bound)	27 May 7 Jun						
Minimum (2.5 % Bound)	17 Aug 29 Aug						
Minimum	19 7 Sep	8 Sep	1 Sep	9 Sep	8 Sep	21 Sep	21 Sep
Minimum (97.5% Bound)	18 4 Oct						

1 Table 2. Same as Table 1, but for GRACE-~~LM~~ and MAR v3.5.2 + ISSM (with Gaussian
 2 spatial and temporal filtering), for the period ~~January~~ 2003 – ~~December~~ -2012.

	MAR v3.5.2 + ISSM	GRACE (median and 95% CI)	GRACE (median and 95% CI, detrended)	MAR v3.5.2 (detrended)
Maximum (2.5% Bound)		5-Mar <u>22 Feb</u>	211 <u>14</u> Mar	
Maximum	21 Apr	25 Mar	199 Apr	1 May
Maximum (97.5% Bound)		22-Apr <u>2 May</u>	24 <u>1</u> May	
Minimum (2.5 % Bound)		477 Sep	29 Aug <u>9 Sep</u>	
Minimum	2 Oct	34 Oct	22 Sep	21 Sep
Minimum (97.5% Bound)		27-Nov <u>7 Dec</u>	188 Oct	

3
4
5
6
7

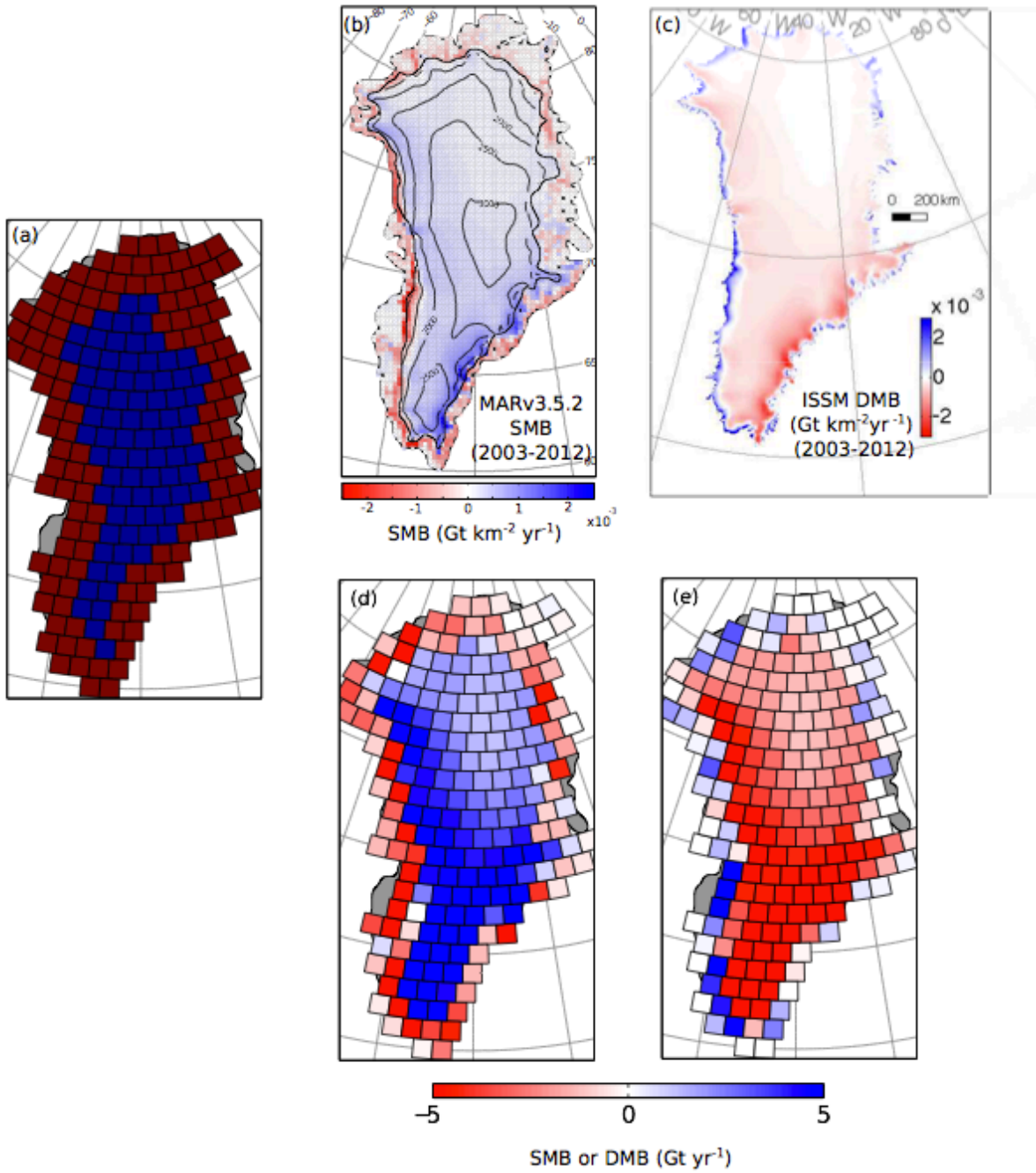


Figure 1. (a) Grid of mascons over the GrIS and constraint regions for the GRACE solution of Luthcke et al. (2013). Areas below 2000 m in elevation are red, while areas above 2000 m are blue. (b) MAR v3.5.2 average specific Surface Mass Balance (SMB, $\text{Gt km}^{-2} \text{yr}^{-1}$) for January 2003 – December 2012 on the MAR grid, for the GrIS and periphery (contours show elevation above sea level). (c) ISSM average specific Dynamic Mass Balance (DMB, $\text{Gt km}^{-2} \text{yr}^{-1}$) for the same period on the ISSM mesh. SMB and DMB for the 2003-2012 period

1 | aggregated to the GRACE-LM grid (without filtering) are also shown for MAR v3.5.2 (d),
2 | and ISSM (e).
3 |

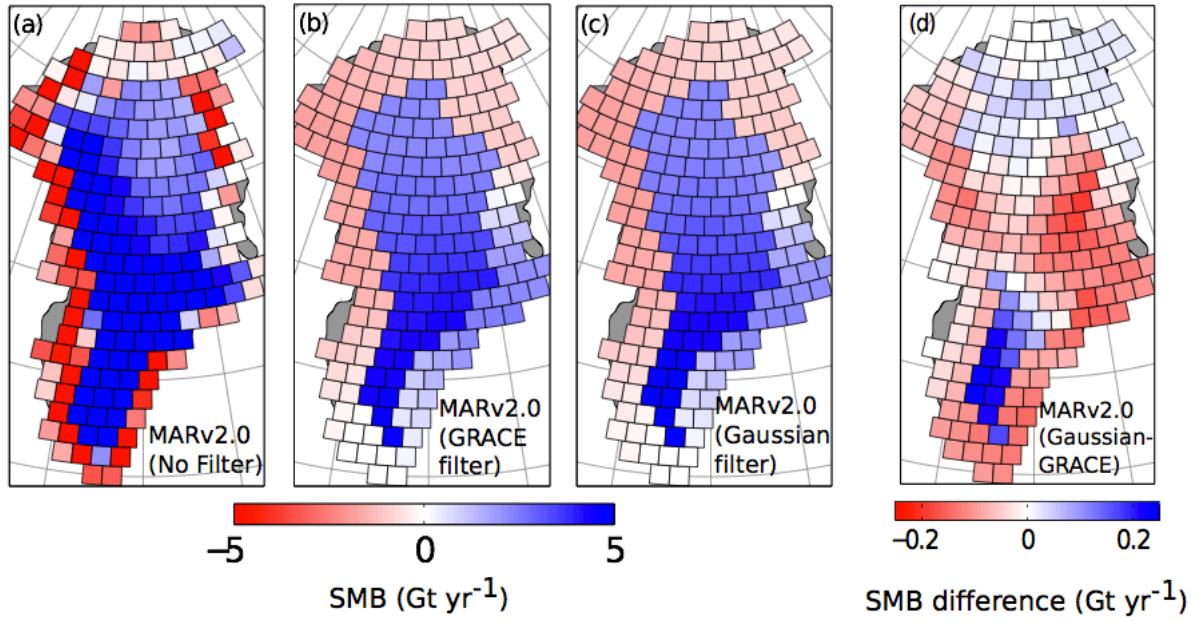


Figure 2. Average MAR v2.0 SMB (Gt yr⁻¹) for the period January 2003 – December 2010: (a) averaged onto GRACE-LM mascons with no filtering, (b) filtered using the resolution operator from GRACE-LM processing, (c) filtered using a Gaussian approximation to GRACE-LM filtering in space and time. (d) The difference between (a) and (b). Note the difference in color scale for (d).

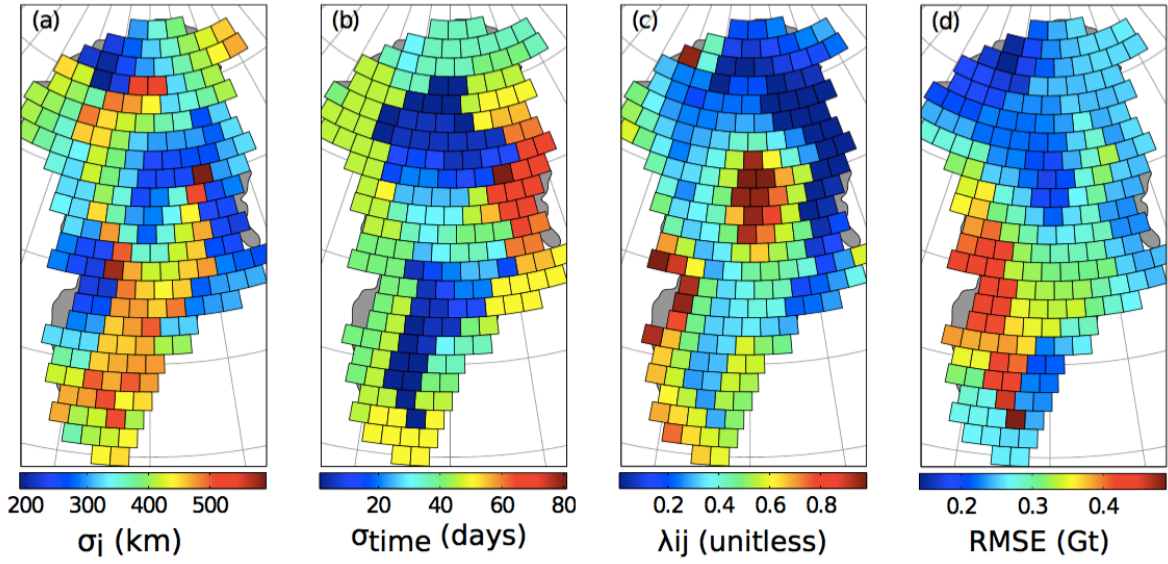


Figure 3. Optimal values of parameters used in spatial and temporal Gaussian filtering of MAR v3.5.2 and ISSM data: (a) the spatial Gaussian radius, (b) the temporal gaussian radius, and (c) the leakage parameter. (d) RSM_{ED} (Gt) for GRACE-LM-filtered vs. Gaussian-filtered MAR v2.0 (January 2003 – December 2010).

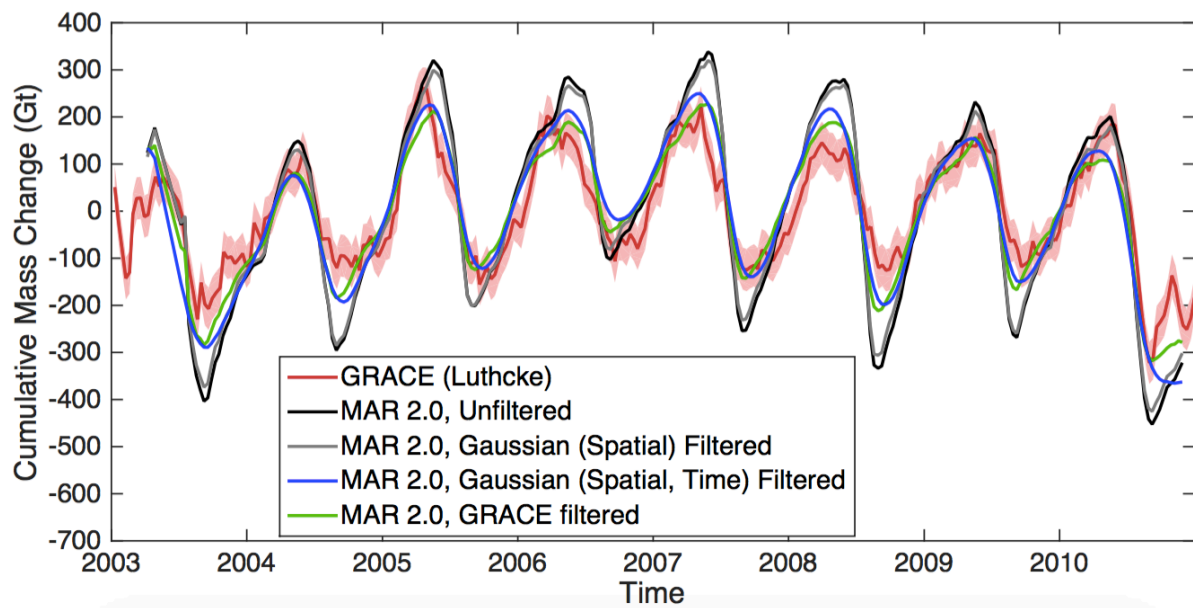


Figure 4. Detrended timeseries of cumulative GrIS-wide mass change, for GRACE-LM, MAR v2.0 (unfiltered), MAR v2.0 (GRACE-LM-filtered), and MAR v2.0 (Gaussian-filtered) for January 2003 – December 2010. In this case a temporal filter has not been applied in the case of Gaussian filtering. Timeseries are shown for Gaussian filtered MAR v2.0 outputs subject to only spatial filtering (gray curve) and both spatial and temporal filtering (blue curve). The pink shading indicates the range of error for the GRACE-LM timeseries.

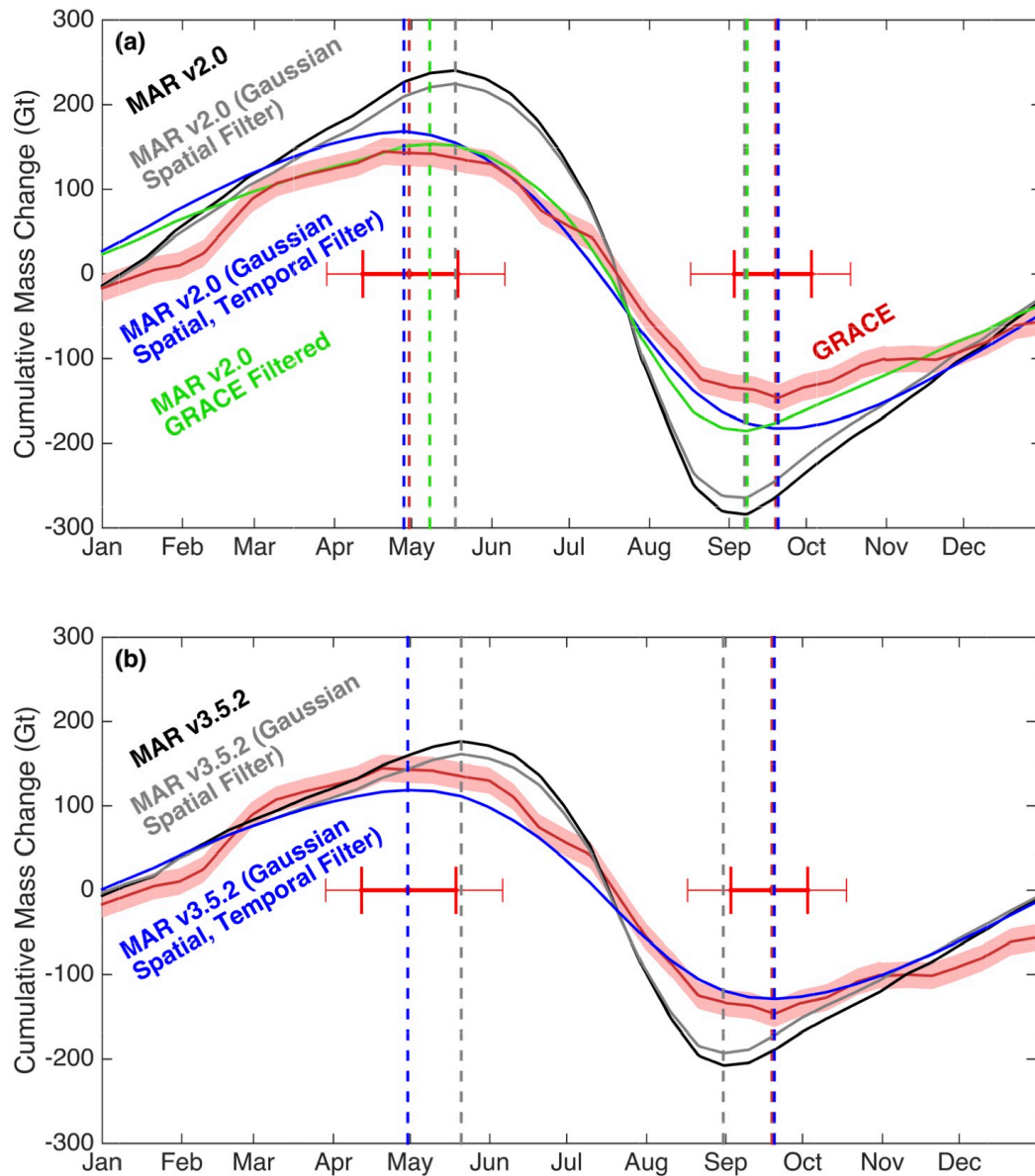


Figure 5. Average seasonal cycle of January 2003 – December 2010 GrIS-wide de-trended cumulative mass change (a) for GRACE-LM, unfiltered MAR v2.0 data, GRACE-LM-filtered MAR v2.0 data, and Gaussian-filtered MAR v2.0 data (with spatial filtering and spatial+temporal filtering). (b) The same as (a), for MAR v3.5.2 (for which GRACE-LM-filtered data are not available). Vertical dashed lines indicate the timing of peaks of maximum and minimum mass in the cycle. Red horizontal error bars indicate the error in the timing of the GRACE cycle. Bold error bars indicate 50% of the GRACE-LM distribution, and thin red lines indicate 95% of the distribution. The error bars have been extended for 10 days in either direction to account for errors associated with temporal resolution.

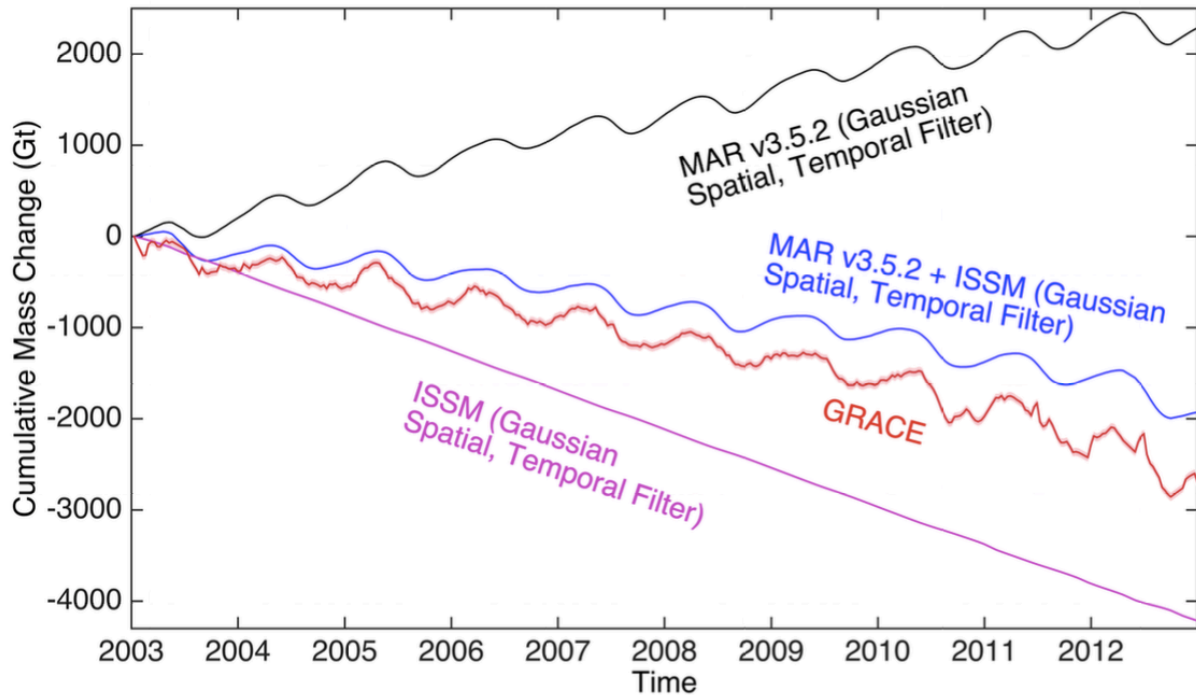


Figure 6. Cumulative GrIS mass change for the January 2003 – December 2012 period from GRACE-LM, MAR SMB, ISSM DMB, and the combined results of MAR v3.5.2 + ISSM. Spatial and temporal Gaussian filtering is applied to model outputs. The estimated error associated with the GRACE-LM solution is small relative to the overall trend, and is denoted with pink shading surrounding the GRACE-LM timeseries. Pink shading surrounding the GRACE timeseries indicates the estimated error associated with the GRACE solution.

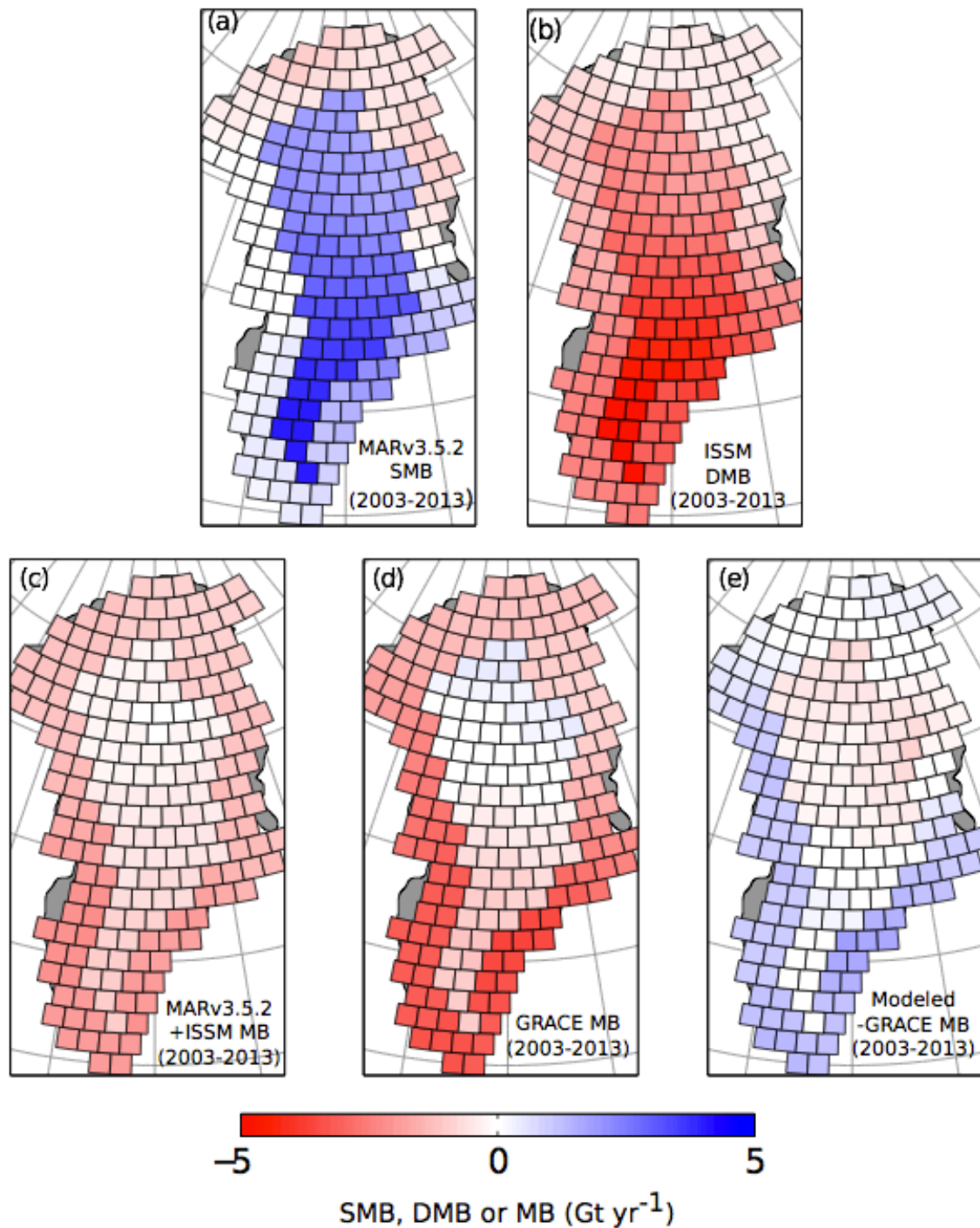


Figure 7. Average January 2003 – December -2012 mass balance (Gt) for MAR, ISSM and GRACE-LM. Gaussian spatial and temporal filtering have been applied to MAR and ISSM outputs. (a) SMB from MAR, (b) Dynamic mass change from ISSM, (c) The sum of (a) and (b), giving the mean MB. GRACE-LM mean MB is shown in (d), and (e) depicts the difference between modeled MB (c) and GRACE-LM MB (d).

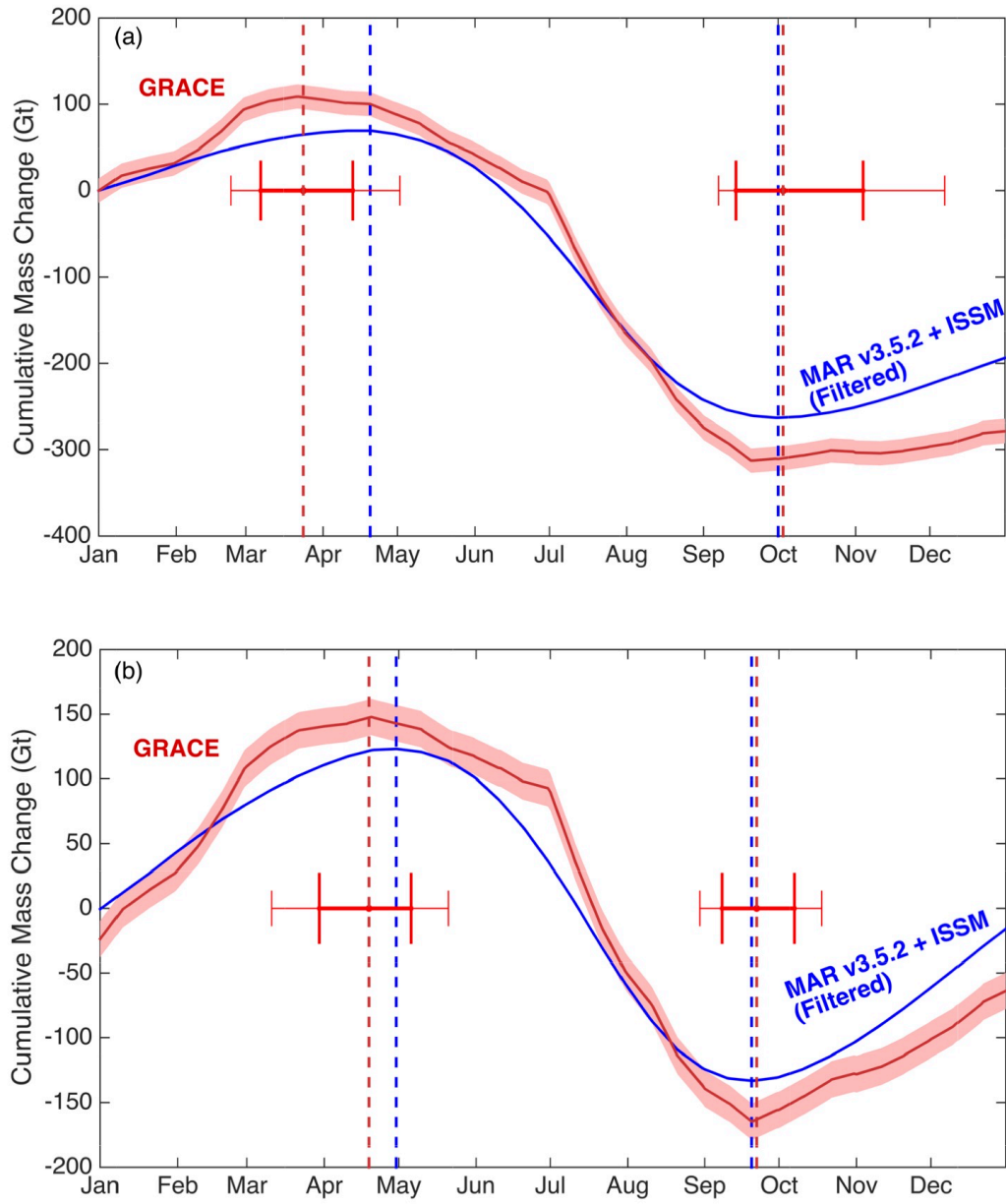


Figure 8. (a) The mean January 2003 – December -2012 seasonal cycle of GrIS cumulative mass change from GRACE-LM and MAR v3.5.2 + ISSM. (b) The same as (a) for the case when the timeseries from all mascons are detrended.

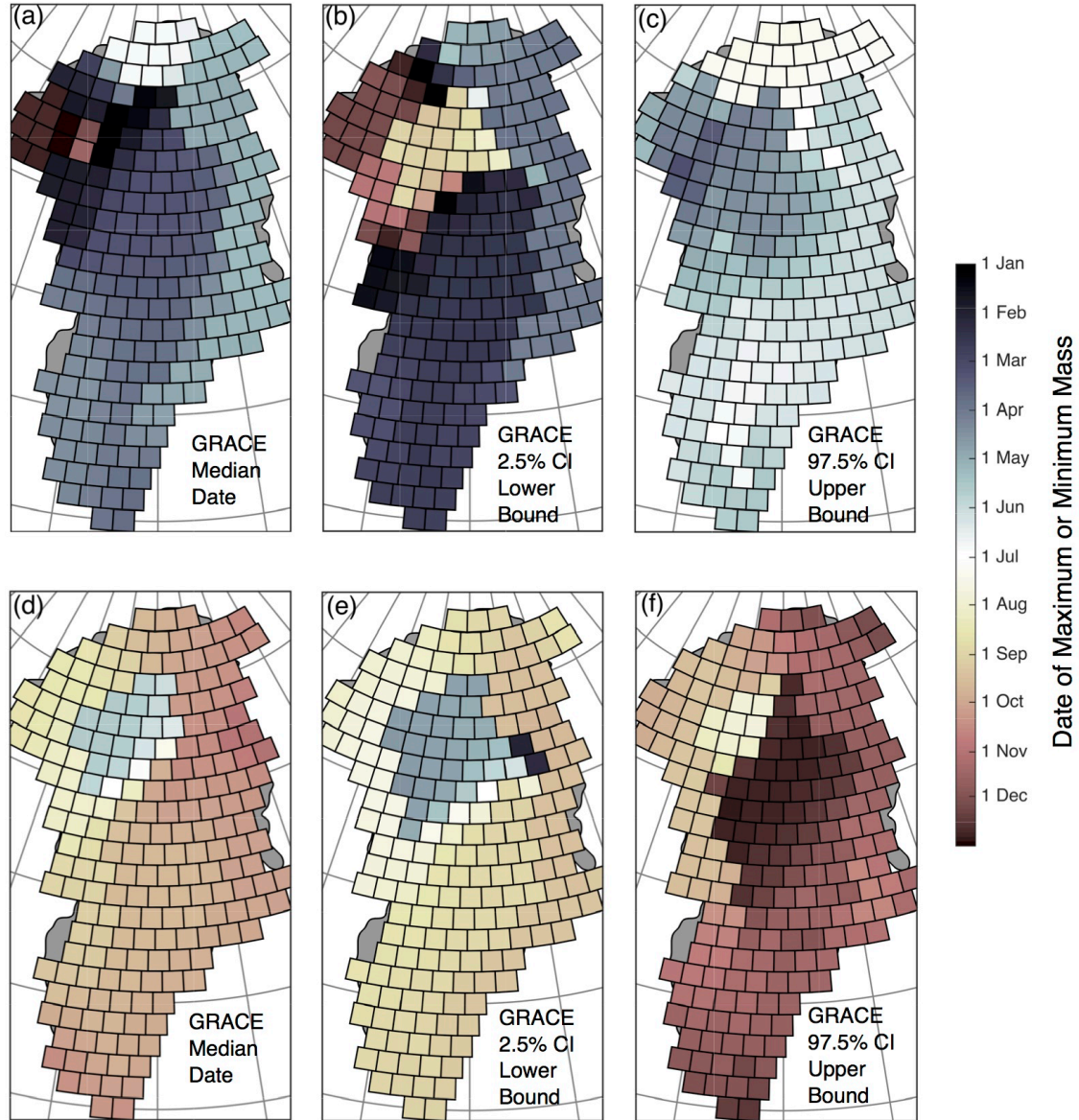


Figure 9. Timing of peaks in the average January 2003 – December -2012 seasonal cycle of detrended cumulative mass from GRACE-LM. (a) Dates of maximum mass for each mascon from the median of the distribution from GRACE-LM (b) the 2.5% limit on the distribution of maximum mass dates, and (c) the 97.5% limit. (d) Dates of minimum mass for each mascon, and (e) the 2.5% and (f) 97.5% limits. 10 days have been subtracted (added) to the lower (upper) bound on the distributions to account for potential errors associated with temporal resolution.

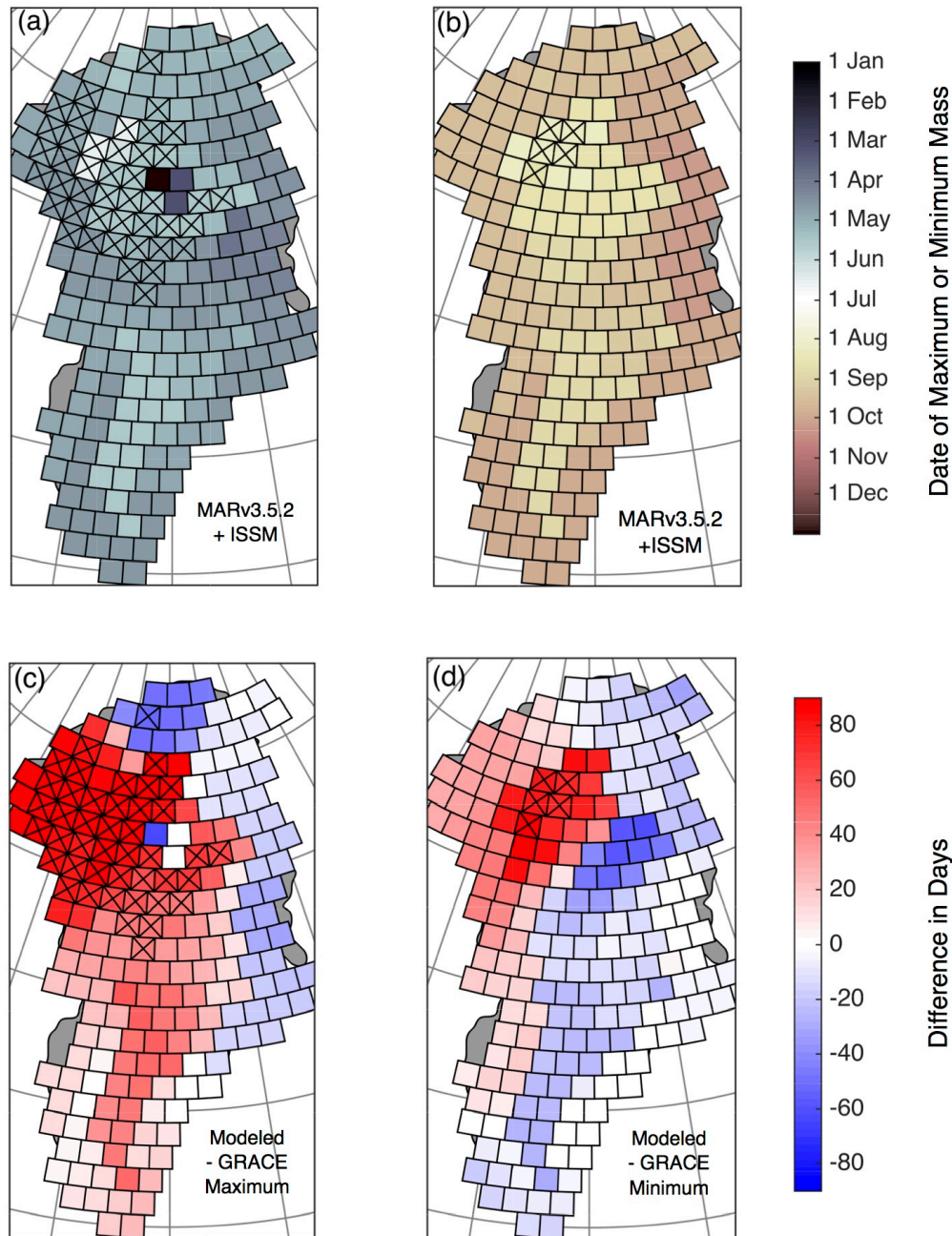


Figure 10. Timing in peaks of the seasonal cycle of de-trended cumulative MB simulated by GRACE-LM-filtered MAR v3.5.2+ISSM outputs. (a) The timing of the maximum peak for each mascon, and (b) the timing of the minimum peak for each mascon. The number of days between MAR v3.5.2 + ISSM and the GRACE-LM median dates for the cycle maximum and minimum are shown in (c) and (d) respectively. For (c) and (d) red colors indicate that the model date occurs later than that of GRACE-LM, and blue colors indicate an earlier date. 'x' marks indicate where the modeled peak falls outside of the 95th percentile range of dates for the GRACE-LM peak shown in Fig.9.

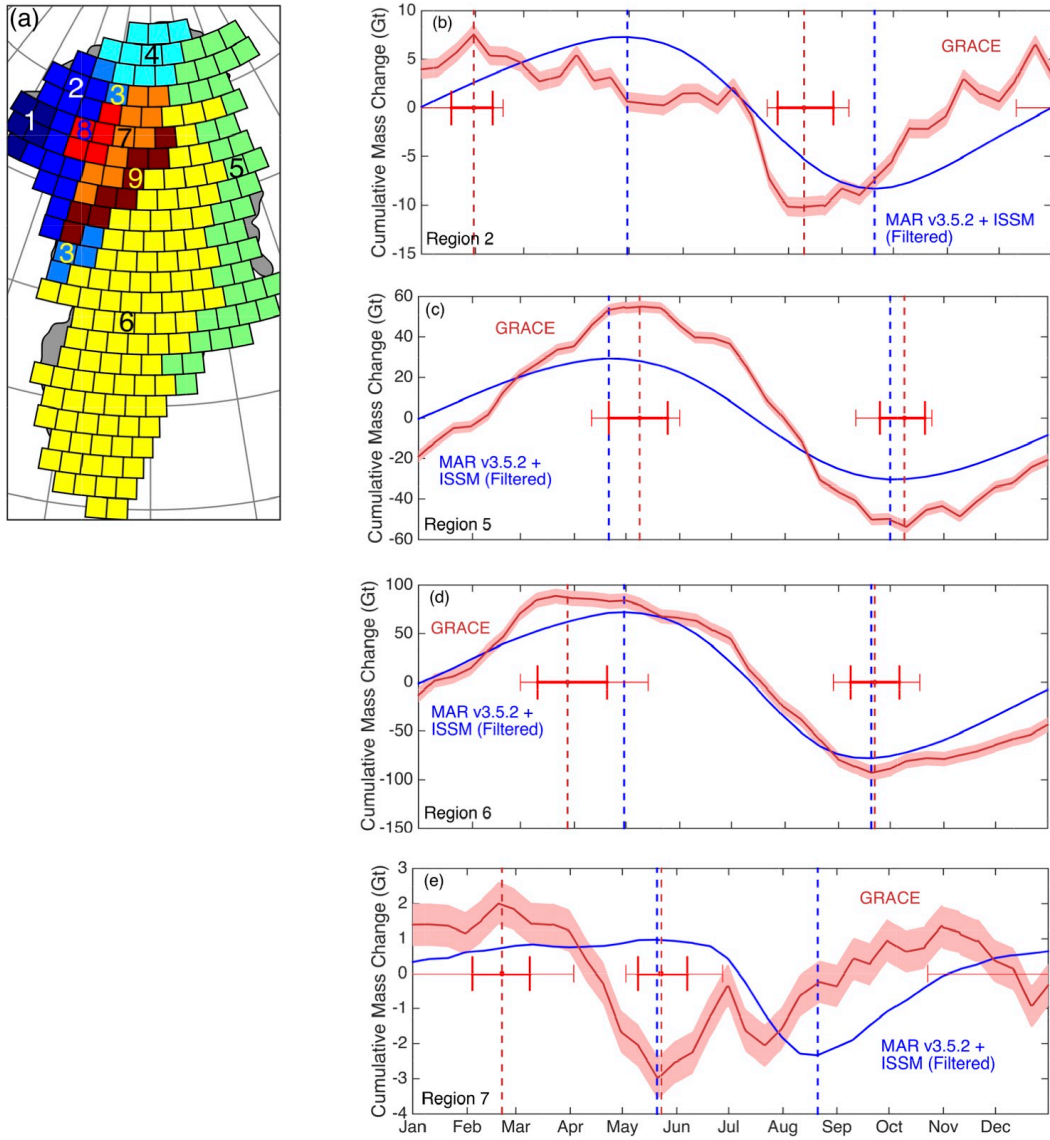
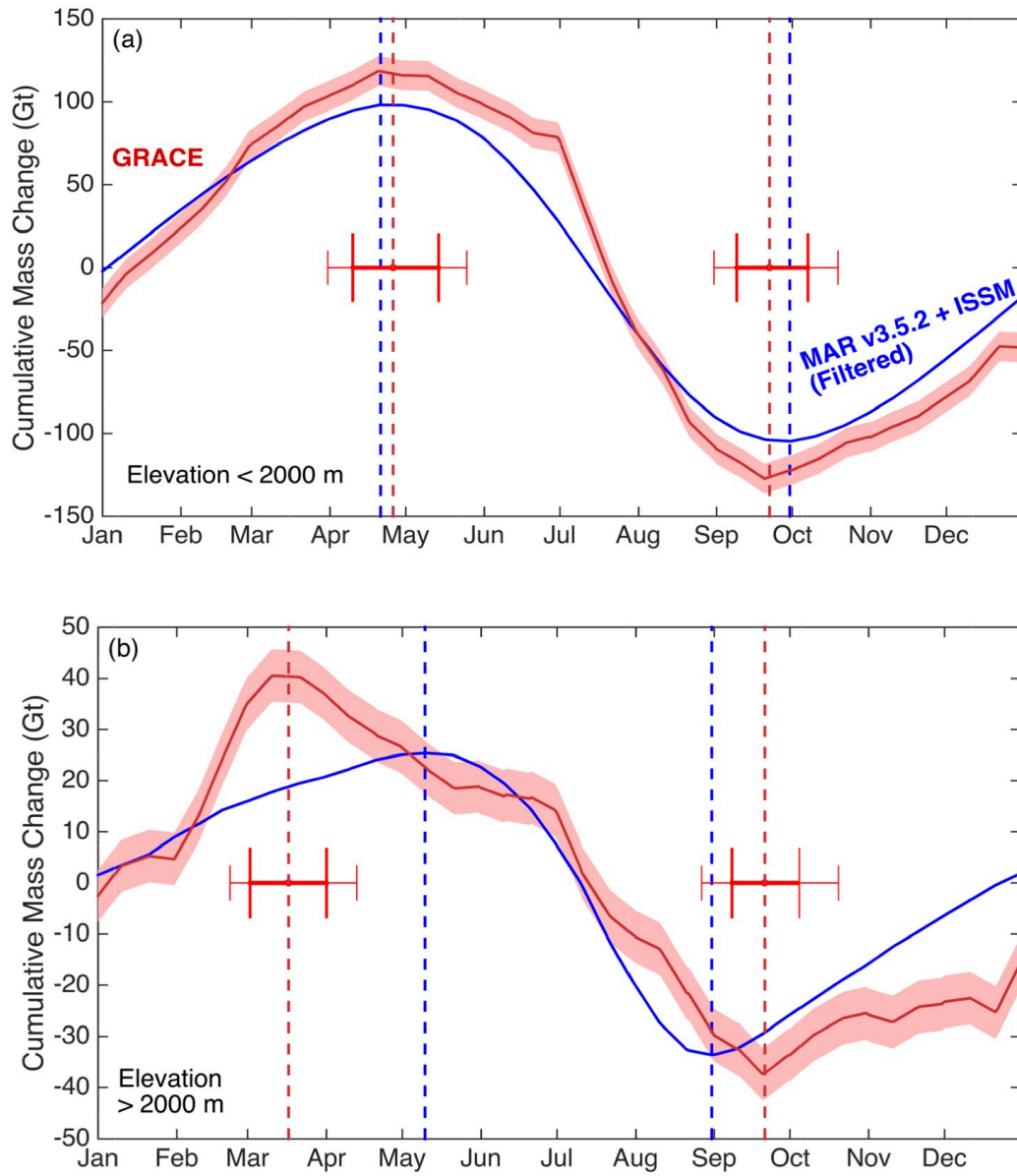


Figure 11. (a) GrIS regions defined based on the timing of peaks in the average cycle of detrended cumulative mass change from GRACE-LM. Also shown is the average seasonal cycle from MAR v3.5.2 + ISSM and GRACE-LM for selected regions: (b) Region 2, (c) Region 5, (d) Region 6, and (e) Region 7.

1



2

3 Figure 12. Same as Fig. 8b, but for (a) regions below 2000 m in elevation, and (b) above 2000
 4 m in elevation.

Table S1. Timing of the seasonal cycle maximum and minimum for cumulative mass change (January 2003 – December -2012) for GRACE-LM, MAR v3.5.2, ISSM forced by MAR v3.5.2, and MAR v3.5.2 + ISSM, within the different regions of the ice sheet defined in Figure 12a, as well as the high (above 2000 m) and low (below 2000 m) elevation regions defined in Figure 1a. The 2.5 % and 97.5% bounds and median value for GRACE-LM are provided.

	< 2000 m	>2000 m	Reg 1	Reg 2	Reg 3	Reg 4	Reg 5	Reg 6	Reg 7	Reg 8	Reg 9
Maximum:											
GRACE (2.5 %)	10 Apr	3 Mar	10 Dec	11 Dec	21 Jan	16 Jun	11 Apr	1 Mar	23 Oct	2 Oct	6 Feb
GRACE median	26 Apr	17 Mar	22 Dec	31 Jan	29 Mar	30 Jun	9 May	28 Mar	21 Feb	11 Nov	8 Mar
GRACE (97.5%)	24 Mar	3 Apr	4 Jan	17 Feb	25 Apr	12 Jul	1 Jun	14 May	3 Apr	28 Feb	5 Apr
MAR v3.5.2	30 Apr	11 May	30 Apr	30 Apr	30 Apr	10 May	21 Apr	30 Apr	21 May	10 Jun	10 May
MAR v3.5.2 + ISSM	21 Apr	10 May	30 Apr	30 Apr	30 Apr	10 May	21 Apr	30 Apr	21 May	10 Jun	1 May
ISSM	21 Oct	1 Oct	10 Oct	10 Oct	1 Oct	1 Oct	21 Oct	10 Oct	1 Oct	10 Sep	1 Oct
Minimum:											
GRACE (2.5 %)	10 Sep	6 Sep	1 Aug	20 Jul	22 Jul	6 Sep	11 Sep	29 Aug	3 May	25 Apr	8 Jul
GRACE median	22 Sep	21 Sep	20 Aug	10 Aug	31 Aug	23 Sep	9 Oct	22 Sep	23 May	19 May	29 Jul
GRACE (97.5%)	9 Oct	10 Oct	3 Sep	5 Sep	25 Sep	18 Oct	25 Oct	18 Oct	28 Jun	18 Jun	17 Sep
MAR v3.5.2	30 Sep	31 Aug	20 Sep	20 Sep	20 Sep	20 Sep	1 Oct	20 Sep	21 Aug	11 Aug	1 Sep
MAR v3.5.2 + ISSM	30 Sep	31 Aug	20 Sep	20 Sep	20 Sep	20 Sep	1 Oct	20 Sep	21 Aug	11 Aug	31 Aug
ISSM	1 Jun	20 Jun	21 May	22 May	10 Jun	22 May	1 Jun	10 Jun	1 Jun	1 Jun	1 Jun

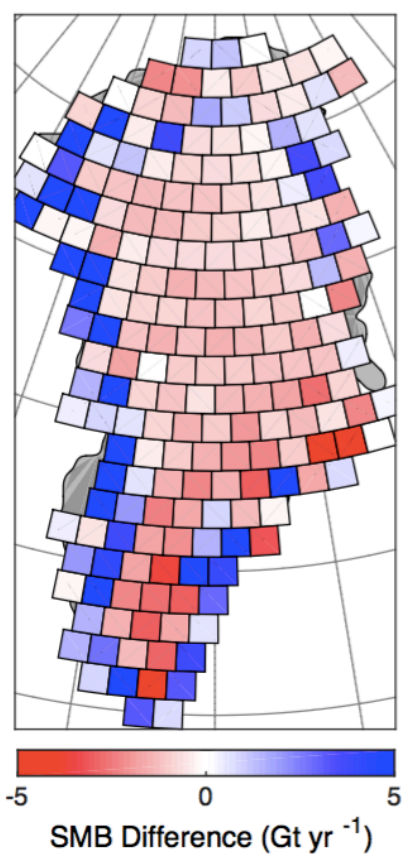


Figure S1. MAR v3.5.2 – MAR v2.0 average SMB, aggregated to the GRACE-LM grid, with no filtering applied, for the period January 2003 – December -2010.

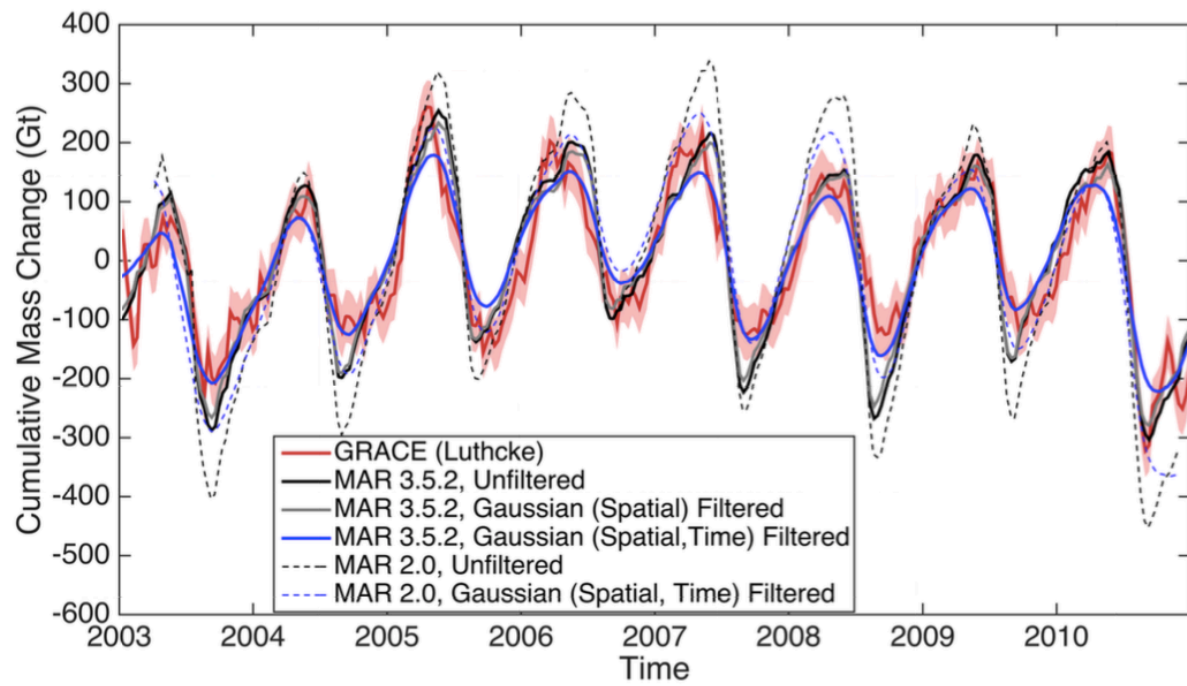


Figure S2: Same as Figure 4, but for MAR v3.5.2. Dashed lines show the MAR v2.0 detrended unfiltered and Gaussian-filtered timeseries for comparison with MAR v3.5.2.

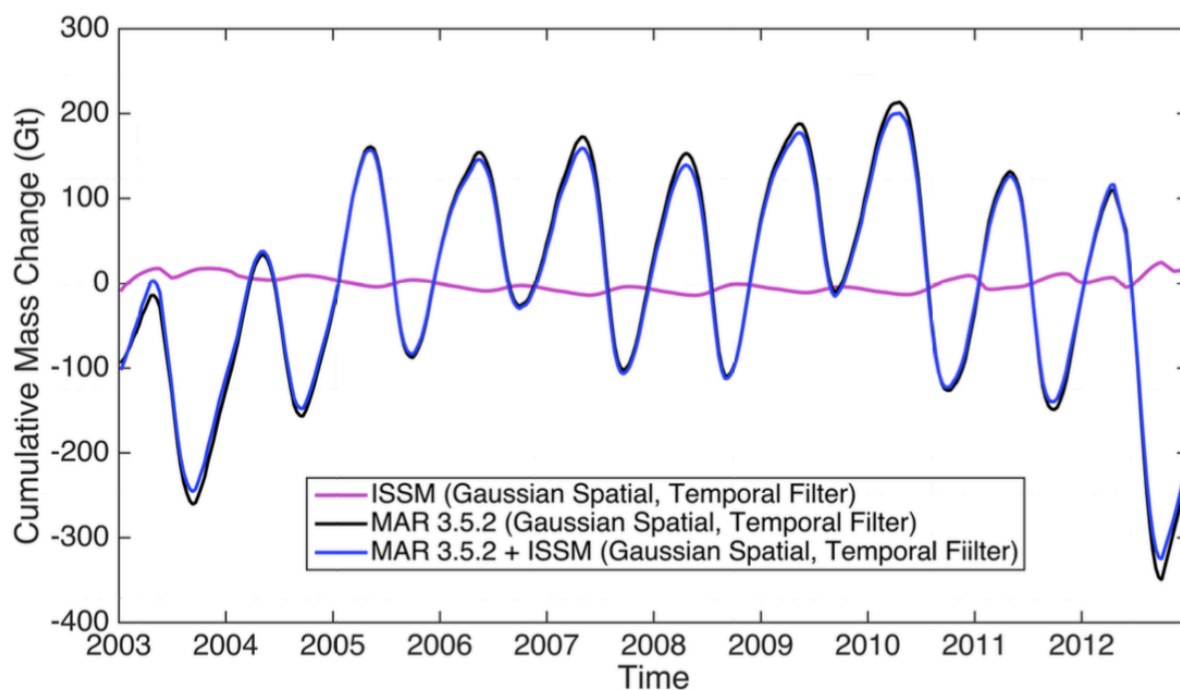


Figure S3: Detrended cumulative timeseries of Greenland mass change for MAR v3.5.2, ISSM, and MAR v3.5.2 + ISSM. Spatial and temporal Gaussian filtering has been applied to the model outputs.

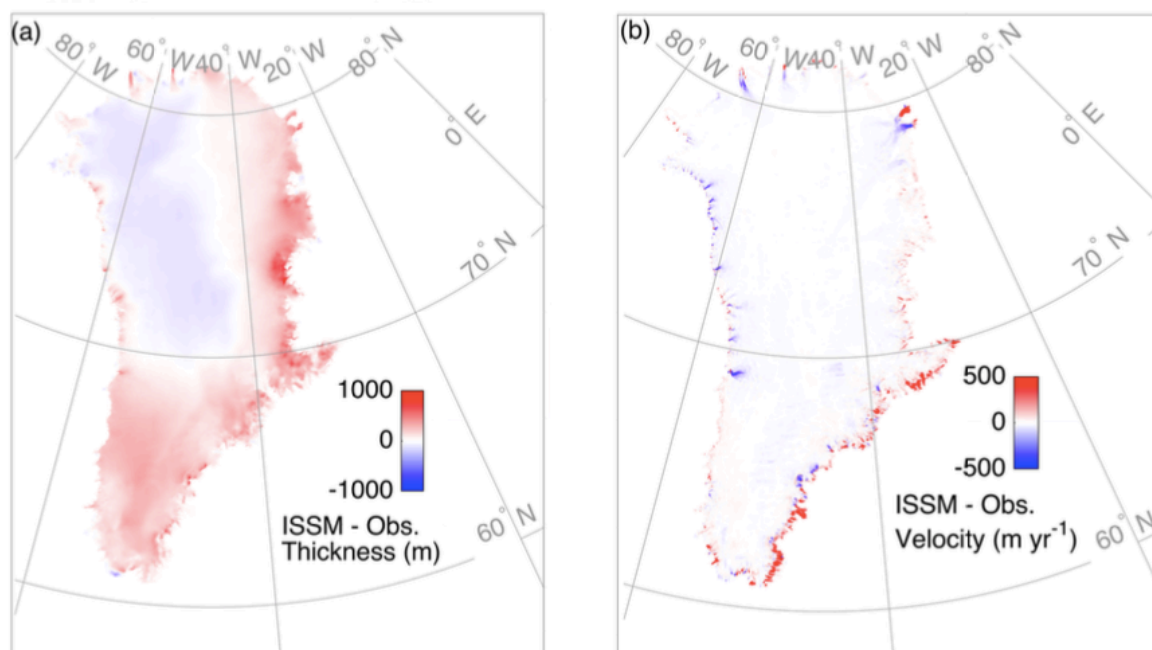


Figure S4: Difference between ISSM and observations for (a) Greenland Ice Sheet thickness (m), and (b) Annual ice velocities, for the year 2003. Thicknesses are obtained from Morlighem et al. (2015), and velocities are those of Rignot et al. (2012).

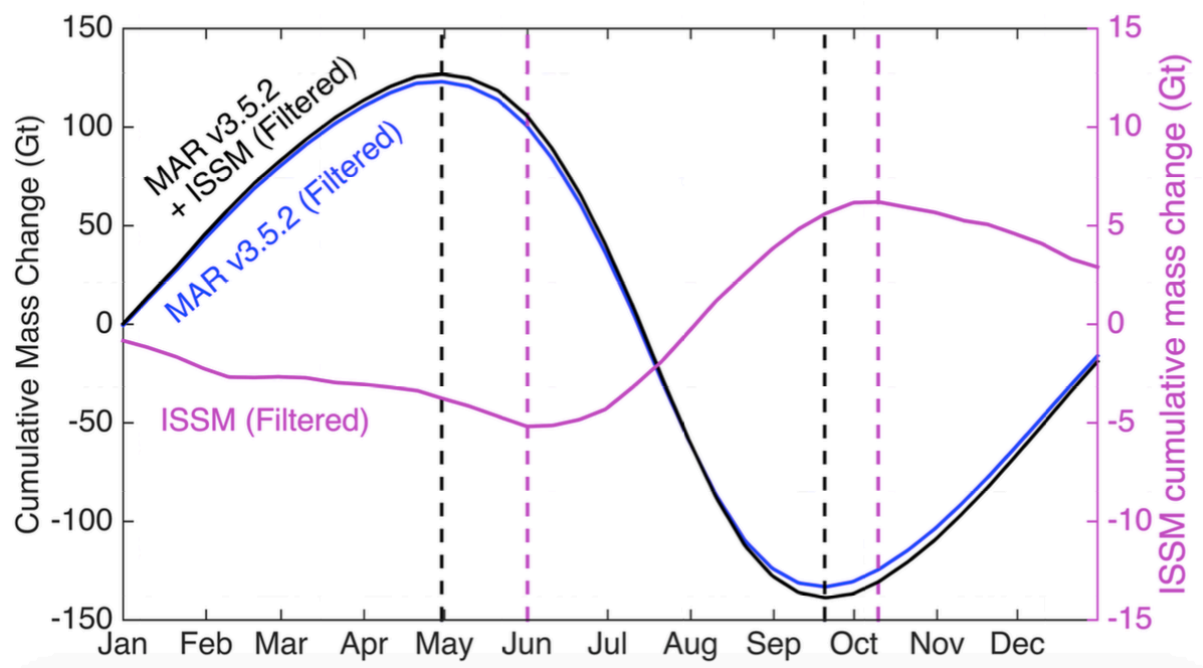


Figure S5: Same as Fig. 8b for MARv 3.5.2 + ISSM, MAR v3.5.2 and ISSM. Note a different axis is used for ISSM data.

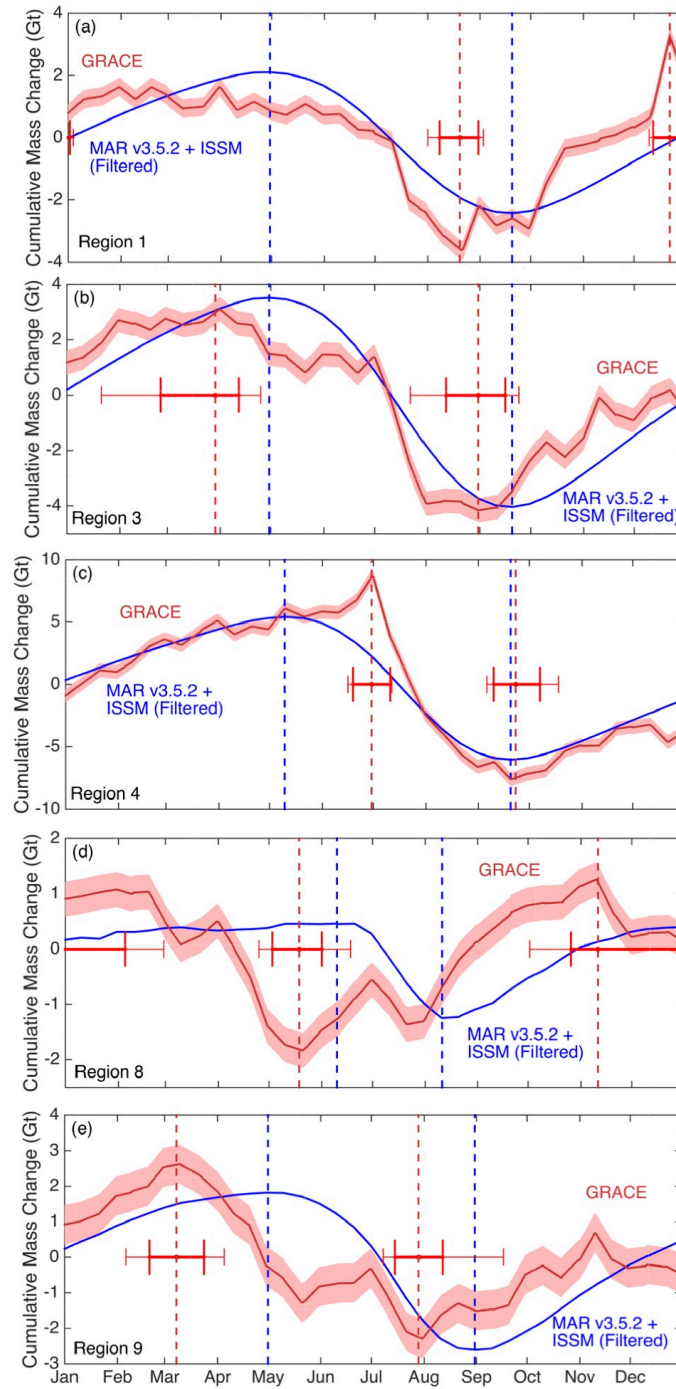


Figure S6: Same as Fig. 11b-e, but for additional regions shown in Fig. 11a: (a) Region 12, (b) Region 3, (c) Region 4, (d) Region 8, and (e) Region 7, ~~(d) Region 8-9~~

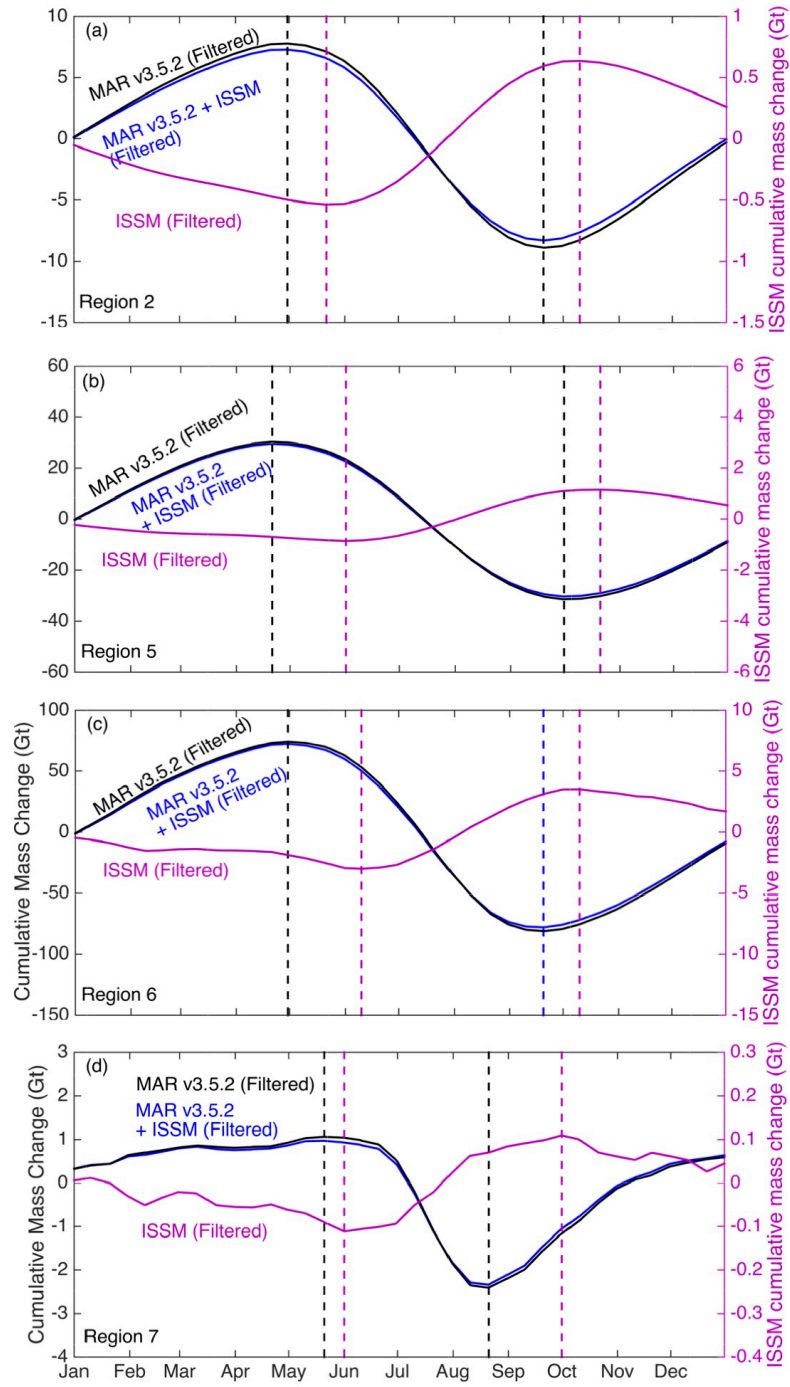


Figure S7: Same as Fig. 11b-e, but showing seasonal cycles for MAR v3.5.2, ISSM and MAR v3.5.2 + ISSM. Note the different axis for ISSM.

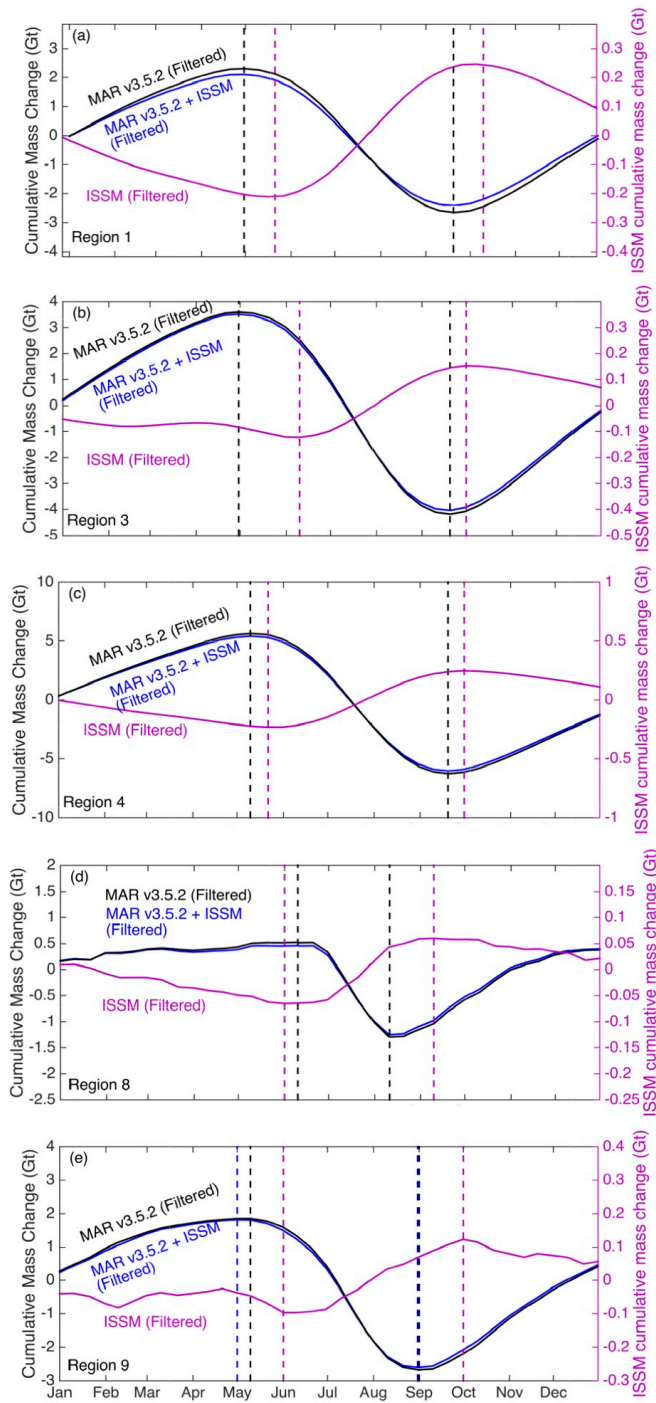


Figure S8: Same as Fig. S6, but showing seasonal cycles for MAR v3.5.2, ISSM and MAR v3.5.2 + ISSM. Note the different axis for ISSM.

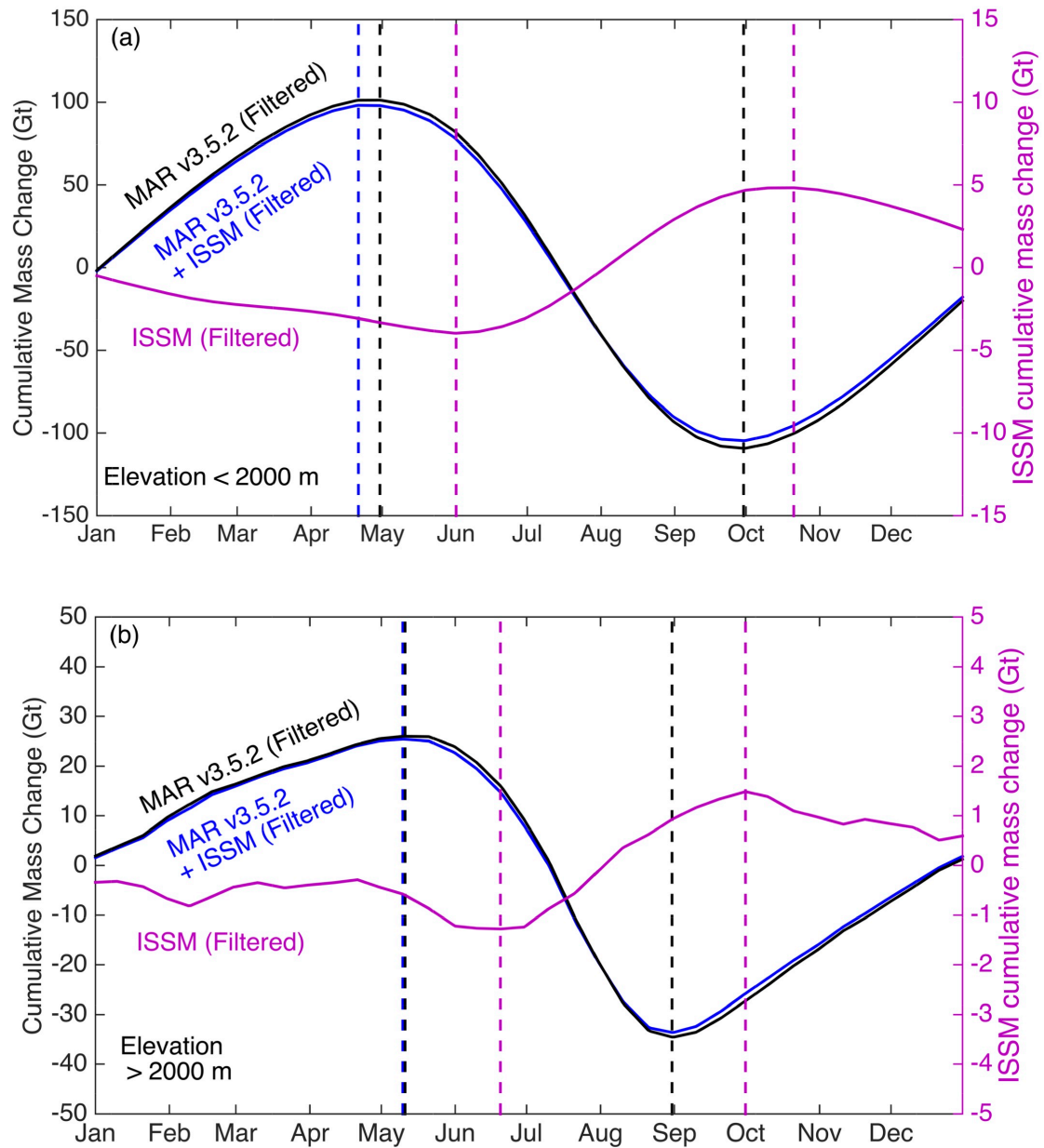


Figure S9: Same as Fig. 12, but showing seasonal cycles for MAR v3.5.2, ISSM and MAR v3.5.2 + ISSM. Note the different axis for ISSM.